

# 1 The coexistence and competition of canonical and comammox nitrite oxidizing 2 bacteria in a nitrifying activated sludge system – experimental observations and 3 simulation studies

4  
5 Mohamad-Javad Mehrani<sup>1</sup>, Przemyslaw Kowal<sup>1</sup>, Dominika Sobotka<sup>1</sup>, Martyna Godzieba<sup>2</sup>, Sławomir  
6 Ciesielski<sup>2</sup>, Jianhua Guo<sup>3</sup>, Jacek Makinia<sup>1\*</sup>

7 <sup>1</sup> Faculty of Civil and Environmental Engineering, Gdansk University of Technology, Narutowicza Street 11/12, 80-233 Gdansk,  
8 Poland

9 <sup>2</sup> Department of Environmental Biotechnology, Department of Environmental Biotechnology, University of Warmia and Mazury  
10 in Olsztyn, Sloneczna 45G, 10-719 Olsztyn, Poland

11 <sup>3</sup> Australian Centre for Water and Environmental Biotechnology (ACWEB, formerly AWMC), The University of Queensland, St.  
12 Lucia, Queensland 4072, Australia

13 \*Correspondence: Jacek Makinia (Email: [jmakinia@pg.edu.pl](mailto:jmakinia@pg.edu.pl), Tel: +48 58 347 19 54, Address: Gdansk University of  
14 Technology, ul. Narutowicza 11/12, 80-233, Gdansk, Poland)

## 15 16 Abstract

17 The second step of nitrification can be mediated by nitrite oxidizing bacteria (NOB), i.e.  
18 *Nitrospira* and *Nitrobacter*, with different characteristics in terms of the r/K theory. In this study,  
19 an activated sludge model was developed to account for competition between two groups of  
20 canonical NOB and comammox bacteria. Heterotrophic denitrification on soluble microbial  
21 products was also incorporated into the model. Four 5-week washout trials were carried out at  
22 dissolved oxygen-limited conditions for different temperatures (12°C vs. 20°C) and main  
23 substrates (NH<sub>4</sub><sup>+</sup>-N vs. NO<sub>2</sub><sup>-</sup>-N). Due to the aggressive reduction of solids retention time (from 4  
24 to 1 d), the biomass concentrations were continuously decreased and stabilized after two weeks at  
25 a level below 400 mg/L. The collected experimental data (N species, biomass concentrations, and  
26 microbiological analyses) were used for model calibration and validation. In addition to the  
27 standard predictions (N species and biomass), the newly developed model also accurately  
28 predicted two microbiological indicators, including the relative abundance of comammox

29 bacteria as well as nitrifiers to heterotrophs ratio. Sankey diagrams revealed that the relative  
30 contributions of specific microbial groups to N conversion pathways were significantly shifted  
31 during the trial. The contribution of comammox did not exceed 5% in the experiments with both  
32  $\text{NH}_4^+$ -N and  $\text{NO}_2^-$ -N substrates. This study contributes to a better understanding of the novel  
33 autotrophic N removal processes (e.g. deammonification) with nitrite as a central intermediate  
34 product.

35

36 **Keywords:** Process Simulation; Comammox; *Nitrospira*; *Nitrobacter*; Two-step nitrification

37

38

39

## 40 1. INTRODUCTION

41 Although nitrification has been known since the end of the 19th century, the process of  
42 understanding has changed dramatically in recent 30 years, which was reflected by evolving  
43 descriptions in the Metcalf and Eddy handbook series (1990, 2003, 2014). The second stage of  
44 nitrification (nitrite oxidation, nitrataion) has been receiving special attention in response to the  
45 development of the novel shortcut nitrogen (N) removal processes, including deammonification  
46 and a shortened pathway of nitrification-denitrification via nitrite (“nitrite shunt”). In those  
47 processes, nitrite is a central component and effective suppression of nitrite oxidizing bacteria  
48 (NOB) is required for successful performance. However, the knowledge of the metabolism of  
49 NOB has been limited and NOB remains a “big unknown of the nitrogen cycle” (Daims et al.,  
50 2016).

51  
52 Traditionally, the genus *Nitrobacter* was considered the typical NOB representative (Metcalf and  
53 Eddy, 1990), whereas more recently the genus *Nitrospira* has been accepted as a more common  
54 NOB population (Metcalf and Eddy, 2014). The dominance of *Nitrospira* in the NOB population  
55 of activated sludge systems has indeed been confirmed in numerous recent laboratory- and full-  
56 scale studies (Keene et al., 2017; Li et al., 2020; Persson et al., 2017; Wu et al., 2019; Zheng et  
57 al., 2019a). Mehrani et al., (2020) presented a comprehensive review study and meta-analysis on  
58 the role of *Nitrospira* in the N removal systems.

59  
60 These two genera (*Nitrobacter* and *Nitrospira*) reveal different characteristics in terms of the r/K  
61 theory. *Nitrobacter* represents the r-strategists which grow faster at high concentrations of the  
62 substrates ( $\text{NO}_2^-$ -N and dissolved oxygen (DO)), whereas *Nitrospira* is the K-strategist with high  
63 substrate affinity at low concentration (Yu et al., 2020). Due to these differences, a more complex



64 suppression strategy would be required for NOB. In general, the controlled solids retention time  
65 (SRT), combined with DO-limited conditions and high residual ammonia, have been  
66 recommended (Regmi et al., 2014). However, low DO conditions ( $<1.0$  mg O<sub>2</sub>/L) can be  
67 inefficient with respect to the suppression of K-strategist *Nitrospira* (Cao et al., 2017).

68  
69 In addition to the competition between *Nitrobacter* and *Nitrospira*, recent findings suggest that  
70 there are other critical issues to be considered for NOB suppression. These issues comprise the  
71 occurrence of different NOB populations, such as *Ca. Nitrotoga* (Kitzinger et al. 2018) and  
72 specific metabolic properties of some microorganisms, such as comammox-*Nitrospira*. In  
73 particular, the discovery of comammox, i.e. complete ammonia oxidation, by a single *Nitrospira*-  
74 type microorganism (Daims et al., 2015; van Kessel et al., 2015) has overturned “a century-old  
75 dogma of nitrification research” (Koch et al., 2019). However, the actual role of comammox  
76 bacteria in full-scale WWTPs is still ambiguous (Koch et al., 2019).

77  
78 The dominance of specific groups of nitrifying bacteria results from selective pressures of the  
79 operational conditions in the bioreactor, including substrate (NH<sub>4</sub><sup>+</sup>-N or NO<sub>2</sub><sup>-</sup>-N) concentration,  
80 DO concentration, and temperature (Metcalf and Eddy, 2014). An efficient approach to the  
81 investigation of the complex nitrifier competition would be a combination of dedicated physical  
82 experiments with advanced microbiological analyses and mathematical modeling. Cao et al.  
83 (2017) noted that the nitrification models should accommodate appropriately the competition  
84 between AOB and NOB to understand factors influencing the competition between autotrophic  
85 N-converting organisms. Two-step nitrification models have been continuously developed for  
86 almost 60 years as summarized by (Mehrani et al., 2022). Such models were used for the  
87 development of suppression strategies for NOB considered collectively as one group (Duan et al.,



88 2019; Kent et al., 2019; Ma et al., 2017; Pérez et al., 2014). Very recent theoretical advances  
89 include the examination of the competition for different r/K strategist groups of AOB and NOB  
90 (Yu et al., 2020; Yin et al., 2022) and the incorporation of comammox in the traditional two-step  
91 model (Mehrani et al., 2021). However, no models have been applied in practice to investigate  
92 the competition of different NOB groups under different substrate (limited vs. unlimited)  
93 conditions.

94

95 The purpose of this study was to develop and validate a model describing the co-existence and  
96 competition between comammox NOB and two groups of canonical NOB, termed NOB1  
97 (*Nitrospira*) and NOB2 (*Nitrobacter*), revealing different r/K characteristics, in response to  
98 decreasing SRTs under different substrate limitation conditions. The experimental data were  
99 collected during four long-term washout experiments carried out at two temperatures (12°C vs.  
100 20°C) with different substrates ( $\text{NH}_4^+\text{-N}$  vs.  $\text{NO}_2^-\text{-N}$ ). The effect of the substrate was also  
101 investigated in terms of the behavior of comammox bacteria. Overall, it was hypothesized that  
102 the newly developed model would provide a better explanation of the competition between the  
103 different NOB groups. Such a model can be a diagnosis and optimization tool for practical  
104 applications of the novel shortcut N removal processes under different  $\text{NO}_2^-\text{-N}$  availabilities.

105

## 106 2. MATERIAL AND METHODS

### 107 2.1. Laboratory experiments and data collection for modeling

#### 108 2.1.1. Long-term washout experiments with different nitrogen substrates

109 Four long-term washout trials were carried out under various laboratory conditions concerning  
110 the nitrogen substrate and temperature (Table 1). For each experiment, new inoculum biomass  
111 samples were obtained from a large municipal wastewater treatment plant (WWTP) in Swarzewo  
112 (180 000 PE), located in northern Poland. The biological part of that plant, performing biological  
113 nutrient removal, consists of six parallel sequencing batch reactors (SBRs). The effluent  
114 standards have been set following the European Union Urban Wastewater Directive (91/21/EEC),  
115 i.e., total N (TN) = 10 mg N/L and total P (TP) = 1 mg P/L.

116  
117 The laboratory experiments were carried out in a fully automated plexiglass SBR with a working  
118 volume of 10 L. The reactor was placed in a thermostatic water bath to keep the temperature  
119 setpoints. Control systems were also installed for aeration and pH. A detailed description of the  
120 laboratory setup can be found elsewhere (Mehrani et al., 2022).

121  
122 In each experiment, the reactor was operated at three cycles per day (8 hours each), including  
123 three phases: feeding (15 minutes), reaction (450 minutes), and decantation (15 minutes). The  
124 latter phase was carried out while mixing, so the solids retention time (SRT) became equal to the  
125 hydraulic retention time. The amount of waste activated sludge (WAS), removed during the  
126 decantation phase, was progressively increasing. This resulted in a gradually decreasing SRT  
127 from the initial 4 d to 1 d at the end of the trial. For all the experiments, the continuous aeration  
128 mode was employed with the DO setpoint of  $0.6 \pm 0.1$  mg/L, while the pH was kept at  $7.5 \pm 0.2$  by  
129 dosing NaOH (2M solution). The temperature setpoints were kept close to the actual process



130 conditions, i.e., 12°C (winter) and 20°C (summer). For a better understanding of the competition  
131 between the NOB groups, the reactor was fed with either  $\text{NH}_4^+\text{-N}$  or  $\text{NO}_2^-\text{-N}$  as the sole inorganic  
132 N substrate. The influent N loadings and detailed feed composition are shown in the SI (Figure  
133 S1 and Table S1, respectively).

134  
135 Mixed liquor samples were collected 3 times per week, then filtered and analyzed for different N  
136 forms, including  $\text{NH}_4^+\text{-N}$ ,  $\text{NO}_3^-\text{-N}$ , and  $\text{NO}_2^-\text{-N}$ , at the initial and the end of the reaction phase.  
137 Mixed liquor suspended solids (MLSS) and mixed liquor volatile suspended solids (MLVSS)  
138 concentrations were analyzed at the initial of the reaction phase. For microbiological analyses,  
139 biomass samples were collected from the reactor in duplicate three times: at the beginning (0 d),  
140 in the middle phase (20 d), and at the end of each trial (35 d). The samples from the initial and  
141 middle phases were transferred to 50 mL Falcon-type tubes for sedimentation and thickening.  
142 The terminal samples, due to the dilution of mixed liquor, were obtained by filtering 5 L of the  
143 effluent through 0.22  $\mu\text{m}$  pore size filters. The biomass samples were stored at -25°C prior to  
144 DNA extraction.

145

146 **Table 1.** Operational parameters and conditions in the reactor during the washout experiments  
147

Trial	Temperature (°C)	pH	DO (mg O <sub>2</sub> /L)	Source of N in the feed	MLSS/MLVSS (mg/L)
T1	20	7.5±0.2	0.6±0.1	$\text{NH}_4^+\text{-N}$	2140/1500
T2	12	7.5±0.2	0.6±0.1	$\text{NH}_4^+\text{-N}$	1890/1450
T3	20	7.5±0.2	0.6±0.1	$\text{NO}_2^-\text{-N}$	1970/1520
T4	12	7.5±0.2	0.6±0.1	$\text{NO}_2^-\text{-N}$	2020/1440

148

149 **2.1.2. Chemical and microbiological analytical methods**

150 The analytical methods used by Dr. Lange and Shimadzu were based on the APHA Standard  
151 Methods (2002). Cuvette tests in a Xion 500 spectrophotometer were used to determine  $\text{NH}_4^+$ -N,  
152  $\text{NO}_3^-$ -N, and  $\text{NO}_2^-$ -N concentrations (Hach Lange, Germany). Before the analysis, mixed liquor  
153 samples were filtered under vacuum pressure using a 1.2 m pore size nitrocellulose filter MFV-3  
154 (Millipore, USA). The gravimetric technique was used to determine the MLSS concentration and  
155 its volatile fraction (MLVSS) in line with the APHA Standard Methods (2002).

156  
157 The DNA extraction was performed followed by FastDNA™ SPIN KIT (MP Biomedicals, USA)  
158 based on the manufacturer's manual. Genomic DNA extracted from the duplicated samples was  
159 pooled together. Following purification, the DNA was utilized for the Illumina Next Generation  
160 Sequencing procedure. Similar to our previous studies (Al-Hazmi et al., 2021), high-throughput  
161 Illumina sequencing of the V3-V4 regions of the 16S rRNA gene procedure and subsequent DNA  
162 sequencing data processing and analysis were carried out.

163

164 **2.2. Organization of the modeling study**

165 The whole modeling study was arranged in five steps as shown in Figure 1, and each step was  
166 described in the following sub-sections.

167



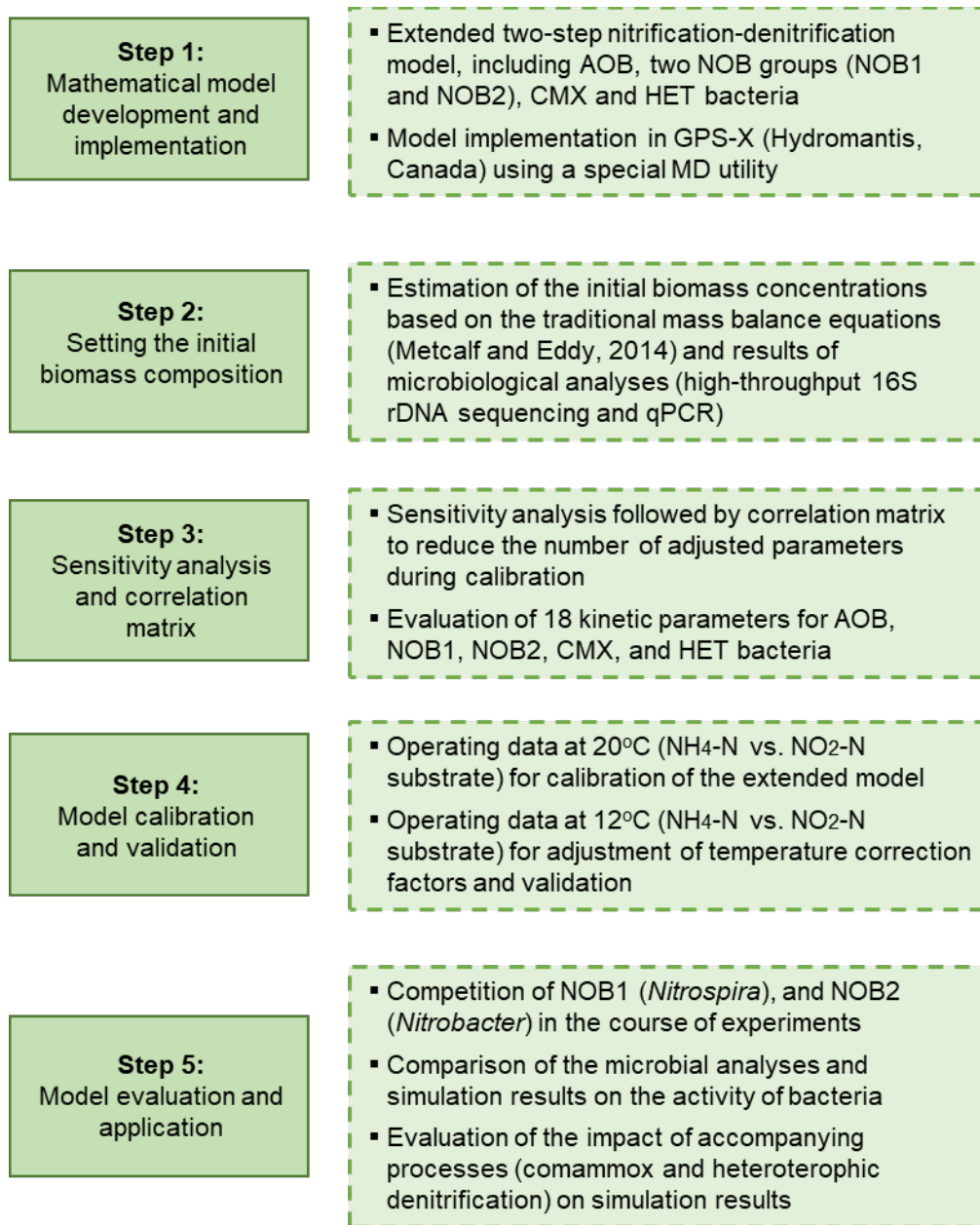


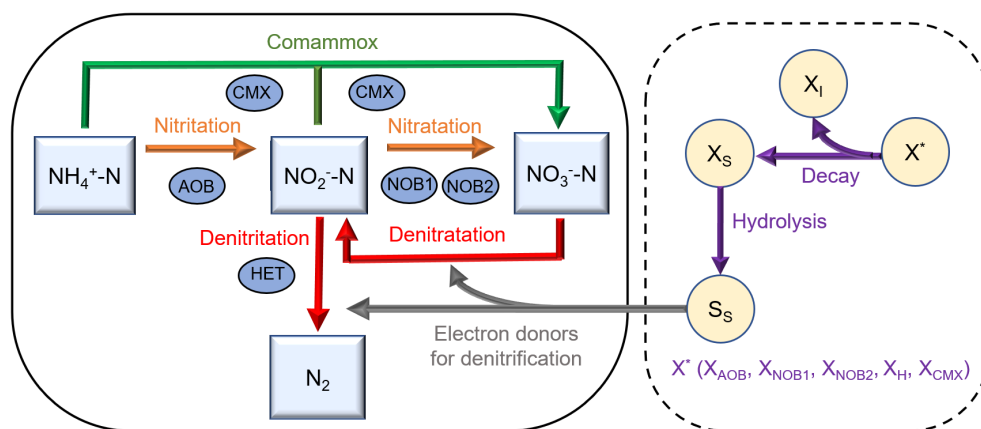
**Figure 1.** Flowchart diagram of the simulation procedure and model application for the competition of two NOB groups and interactions with comammox and heterotrophic denitrification

### 2.2.1. Mathematical model development and implementation

The microbial growth model, used in the present study, was based on the death-regeneration concept from the Activated Sludge Model No. 1 (ASM1) (Henze, 2000). In our previous studies, a two-step nitrification model was developed with further expansions to incorporate comammox (Mehrani et al., 2021) and heterotrophic denitrification on soluble microbial products (SMP)

178 (Mehrani et al., 2022). In the present study, NOB were divided into two subgroups depending on  
 179 their different characteristics in terms of the r/K theory, i.e., *Nitrospira* as K-strategists vs.  
 180 *Nitrobacter* as r-strategists (Figure 2b). Their behavior and competition were assessed during the  
 181 washout experiments under different substrate availabilities (Table 2). It was assumed that the  
 182 substrate affinity is higher for *Nitrobacter* than *Nitrospira* ( $K_{NO_2,NB} > K_{NO_2,NS}$ ) allowing the latter  
 183 to prevail under  $NO_2^-$ -N limited conditions ( $NH_4^+$ -N feeding). On the other hand, *Nitrobacter* can  
 184 outcompete *Nitrospira* under  $NO_2^-$ -N feeding due to a higher maximum specific growth rate  
 185 ( $\mu_{max,NB} > \mu_{max,NS}$ ).

186



187

188 **Figure 2.** A concept of the extended nitrification model considering two NOB groups and interactions with  
 189 comammox and heterotrophic denitrification

190

191 The GPS-X software 8.0 (Hydromantis, Canada) was used as a simulation environment for  
 192 implementing the model and running simulations. Internal GPS-X utilities were used for  
 193 sensitivity analysis (Analyzer) and parameter optimization (Optimizer).

194

195

196

197 **Table 2.** Effect of the substrate conditions (limited vs. unlimited) on the different r/K NOB strategists

NOB substrate availability		<i>Nitrospira</i> (K-strategist)		<i>Nitrobacter</i> (r-strategist)
Limited (NH <sub>4</sub> <sup>+</sup> -N feed)	↑	$\mu_{max,NS} \frac{S_{NO2}}{S_{NO2} + K_{NO2,NS}} \frac{S_O}{S_O + K_{O,NS}}$	↓	$\mu_{max,NB} \frac{S_{NO2}}{S_{NO2} + K_{NO2,NB}} \frac{S_O}{S_O + K_{O,NB}}$
Unlimited (NO <sub>2</sub> <sup>-</sup> -N feed)	↓	$\mu_{max,NS} \frac{S_{NO2}}{S_{NO2} + K_{NO2,NS}} \frac{S_O}{S_O + K_{O,NS}}$	↑	$\mu_{max,NB} \frac{S_{NO2}}{S_{NO2} + K_{NO2,NB}} \frac{S_O}{S_O + K_{O,NB}}$

198

### 199 2.2.2. Setting the initial conditions (biomass composition and model parameters)

200 The mechanistic ASM-type models require a setting of the initial concentrations for specific  
 201 groups of microorganisms. Based on the systematic protocol proposed in the previous study  
 202 (Mehrani et al., 2022), a combination of mass balance calculations and microbiological analyses  
 203 were applied to determine the initial concentrations of AOB, NOB (*Nitrospira*), comammox  
 204 bacteria, and denitrifying heterotrophs. The abundances of *Nitrobacter* were below the detection  
 205 limit in all the initial samples. Therefore, the initial concentrations of these bacteria were set at  
 206 1% of *Nitrospira* initial concentration.

207

208 The initial values of kinetic and stoichiometric parameters were adopted from the literature (Koch  
 209 et al., 2019; Yu et al., 2020; Metcalf and Eddy 2003; Hiatt and Grady, 2008; Roots et al. 2019).  
 210 Subsequently, the kinetic parameters were subjected to sensitivity analysis (see Section 2.3).  
 211 Three kinetic parameters, including K<sub>O</sub> for AOB and NOB1 together with K<sub>NO2</sub> for NOB1, were  
 212 experimentally determined in batch tests (Mehrani et al., 2022). These parameters were not  
 213 further adjusted during model calibration.

214

215

### 2.3. Sensitivity analysis and correlation matrix

Coupling local sensitivity analysis and the development of a correlation matrix allows reducing the number of parameters adjusted during model calibration. The analysis was carried out based on the results from trial T1 ( $\text{NH}_4^+\text{-N}$  substrate) and trial T3 ( $\text{NO}_2^-\text{-N}$  substrate). For trial T1, the different microbial groups (AOB, NOB1, CMX, and HET) were subjected to the sensitivity analysis concerning  $\text{NH}_4^+\text{-N}$ ,  $\text{NO}_3^-\text{-N}$ , and  $\text{NO}_2^-\text{-N}$  behavior. In trial T3, AOB were not considered due to the lack of substrate ( $\text{NH}_4^+\text{-N}$ ) for these bacteria. Instead, NOB2 were included concerning  $\text{NO}_3^-\text{-N}$  and  $\text{NO}_2^-\text{-N}$  behavior. The classification of sensitivity coefficients,  $S_{i,j}$ , (from 0 to  $>2.5$ ) was adopted from a recent study of Cao et al. (2020).

Subsequently, all pairs of the most sensitive kinetic parameters were evaluated by the correlation matrix. If the correlation coefficient for any pair is high enough, the calibration procedure can be simplified by adjusting only one of the two parameters (Zhu et al., 2015).

### 2.4. Model calibration and validation

The results of the trials at 20 °C (T1 and T3) with both substrates ( $\text{NH}_4^+\text{-N}$  vs.  $\text{NO}_2^-\text{-N}$ ) were used for model calibration, while the results of the two trials at 12 °C (T2 and T4) were used for validation. The Nelder-Mead simplex method with the maximum likelihood objective function was used for parameter estimation as described in detail in a previous study (Lu et al. 2019). The model efficiency was assessed using the conventional performance metrics, such as the determination coefficient ( $R^2$ ), root mean square error (RMSE), and mean absolute error (MAE). In addition, the Janus coefficient ( $J^2$ ) was calculated to evaluate a change in the model efficiency between the calibration and validation phases (Hauduc et al., 2015).

## 240 **2.5. Model evaluation and application**

241 After model validation, the competition between two NOB groups (*Nitrospira* and *Nitrobacter*)  
242 under different substrate conditions ( $\text{NH}_4^+\text{-N}$  and  $\text{NO}_2^-\text{N}$ ) was investigated by comparing the  
243 predicted process rates (mg N/L·d) in trials T1 and T3. Sankey diagrams were developed based  
244 on the daily average rates at different phases of the experiment, i.e. 0 d (beginning), 20 d, and 35  
245 d (end). The diagrams were used to identify the dominant N conversion pathways and assess the  
246 effect of the accompanying processes (comammox, heterotrophic denitrification).

247

248

## 249 **3. RESULTS**

### 250 **3.1. Initial biomass composition**

251 In all the trials, the initial MLSS and MLVSS concentrations were approximately 2000 and 1500  
252 mg/L, respectively (Table 1). The calculated initial concentrations of the specific microbial  
253 groups ( $X_{\text{AOB}}$ ,  $X_{\text{NOB}}$ ,  $X_{\text{CMX}}$ ,  $X_{\text{HET}}$ ), estimated sequentially using the systematic protocol of  
254 Mehrani et al. (2022), are shown in the SI (Table S3).

255

### 256 **3.2. Sensitivity analysis and correlation matrix**

257 Figure 3a,c shows the sensitivity coefficients, derived for all 18 kinetic coefficients ( $\mu$ ,  $K$ ,  $b$ ),  
258 which were obtained based on the results from trial T1 ( $\text{NH}_4^+\text{-N}$  substrate) and trial T3 ( $\text{NO}_2^-\text{N}$   
259 substrate). For trial T1, the different microbial groups (AOB, NOB1, CMX, and HET) were  
260 subjected to the sensitivity analysis for the behavior of  $\text{NH}_4^+\text{-N}$ ,  $\text{NO}_3^-\text{N}$ , and  $\text{NO}_2^-\text{N}$ . For trial  
261 T3, NOB2 were considered instead of AOB, and the sensitivity analysis was performed based on  
262 the behavior of  $\text{NO}_3^-\text{N}$  and  $\text{NO}_2^-\text{N}$ .

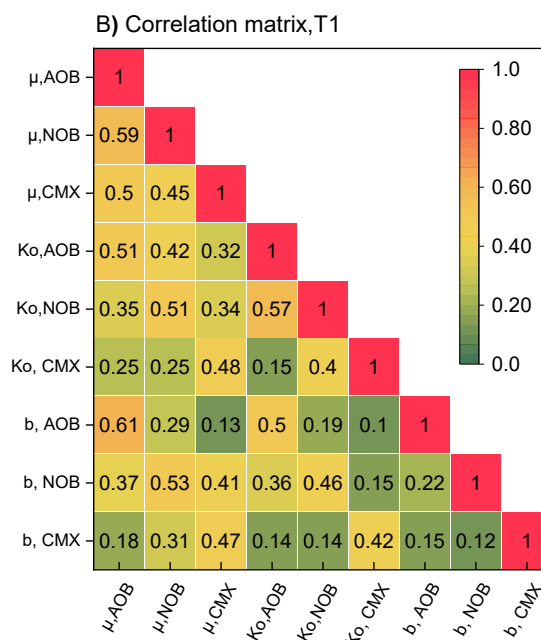
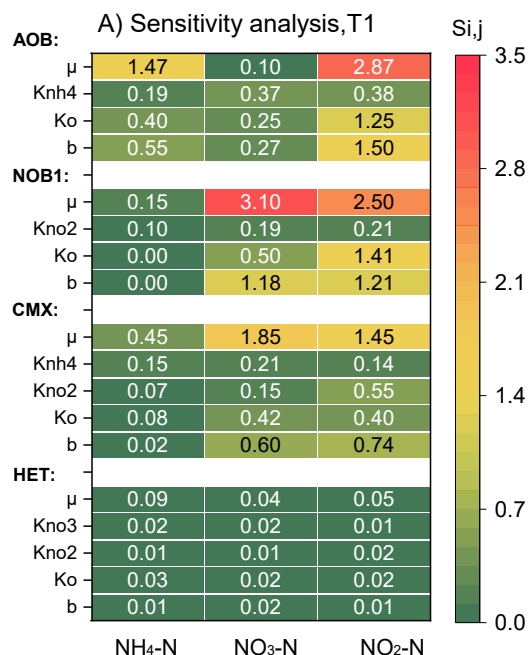
263

264 In general, for trial T1, the very influential coefficients ( $S_{ij} \geq 2$ ) were  $\mu_{AOB}$  and  $\mu_{NOB1}$  concerning  
265 the behavior of  $NO_2^-N$ , and  $\mu_{NOB1}$  associated with the behavior of  $NO_3^-N$ . The  $\mu_{AOB}$  had also a  
266 substantial influence ( $1 \leq S_{ij} < 2$ ) on the behavior of  $NH_4^+N$ , while  $\mu_{CMX}$  was very influential ( $S_{ij}$   
267  $\geq 2$ ) on the  $NO_3^-N$  behavior. The decay rates ( $b_{AOB}$  and  $b_{NOB1}$ ) and DO half-saturation  
268 coefficients ( $K_{OAOB}$  and  $K_{ONOB1}$ ) were influential ( $1 \leq S_{ij} < 2$ ) on the  $NO_2^-N$  behavior.

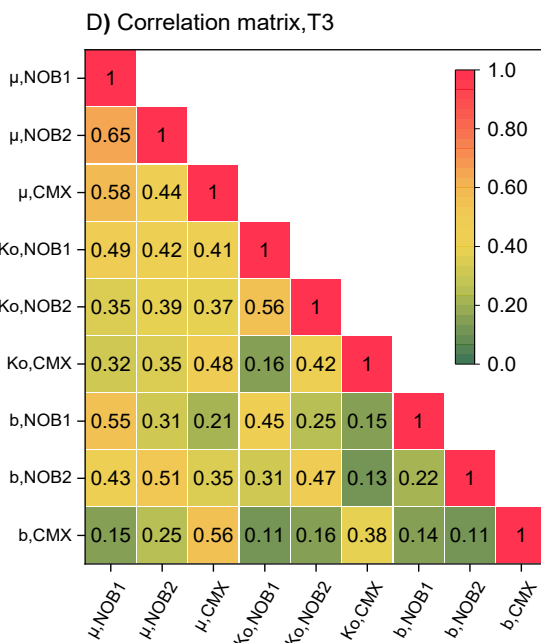
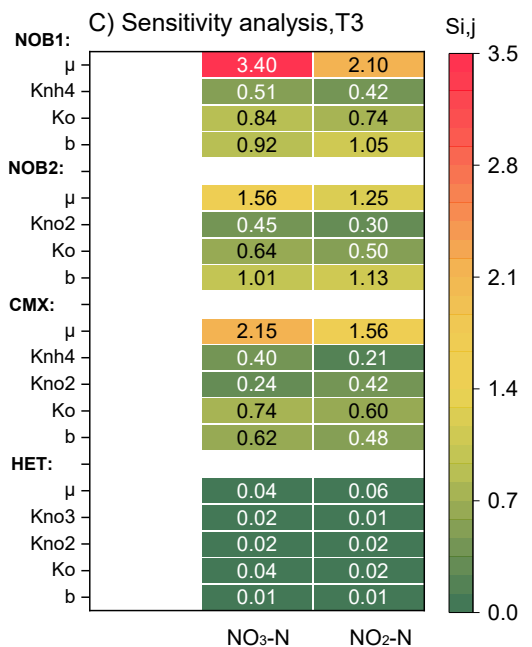
269  
270 For trial T3,  $\mu_{NOB1}$  and  $\mu_{CMX}$  with  $S_{ij} > 2$ , followed by  $\mu_{NOB2}$  with  $S_{ij} = 1.8$ , were the most  
271 influential coefficients associated with the behavior of  $NO_3^-N$ . The decay rates ( $b_{NOB1}$  and  $b_{NOB2}$ )  
272 were also influential ( $S_{ij} > 1$ ) with respect to the behavior of  $NO_2^-N$  and  $NO_3^-N$ .

273  
274 Based on the results of sensitivity analysis for both trials, the very influential kinetic parameters  
275 ( $S_{ij} > 1$ ) were subjected to evaluation by a correlation matrix (Figure 3b,d). In general, the highest  
276 correlation coefficients in both trials referred to the maximum growth rates ( $\mu$ ) and decay  
277 coefficients ( $b$ ) for all the nitrifier groups. Hence, for simplification of the calibration procedure,  
278  $b$  coefficients were omitted in further adjustments.

279



280



281

282

**Figure 3.** Sensitivity coefficients,  $S_{i,j}$ , and correlation matrix for the most sensitive kinetic parameters ( $\mu$ ,  $K$ ,  $b$ ) in

283

trial T1 (A-B) and trial T3 (C-D) (the effect of NOB2 in trial T1 was not considered due to very low sensitivity

284

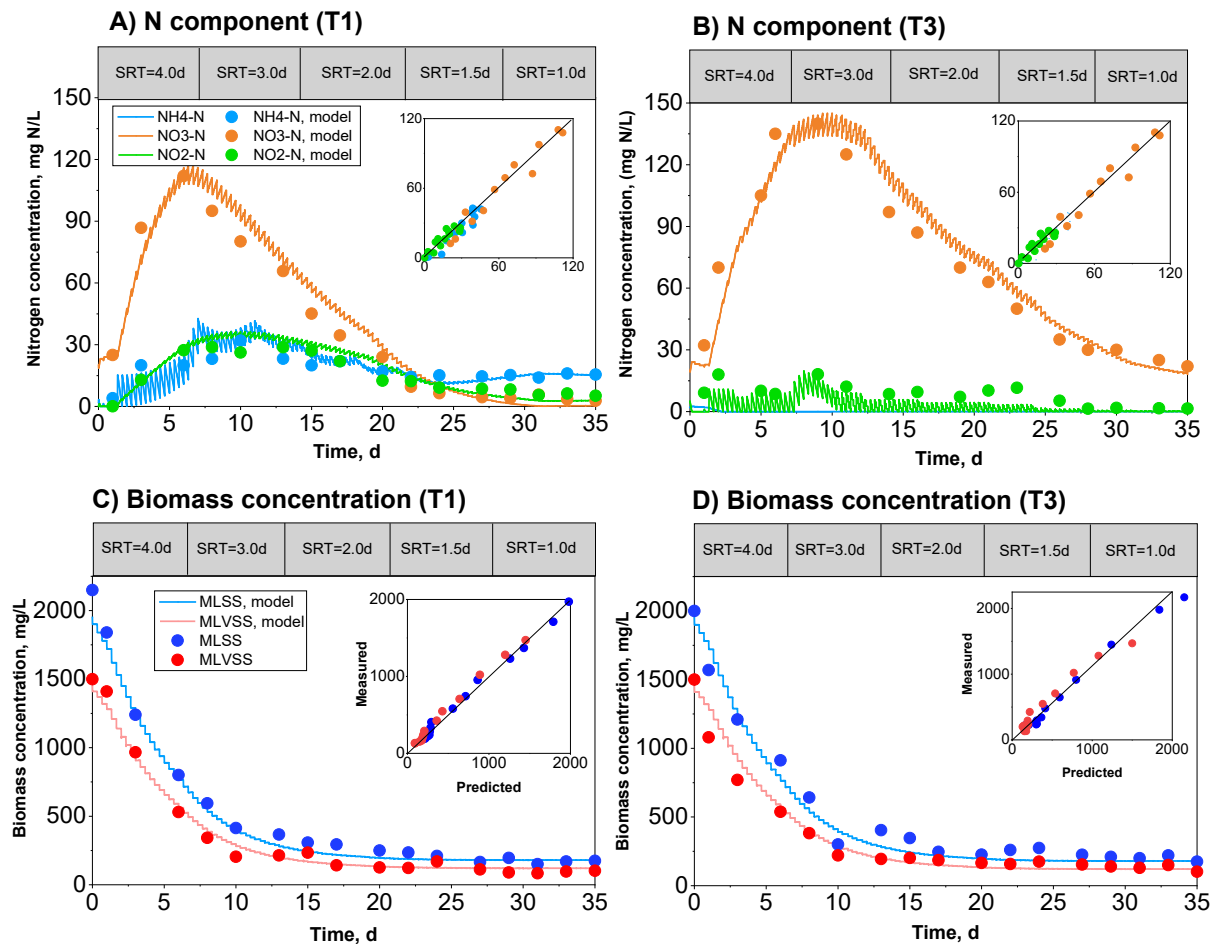
( $S_{i,j} \leq 0.01$ ))

285

286

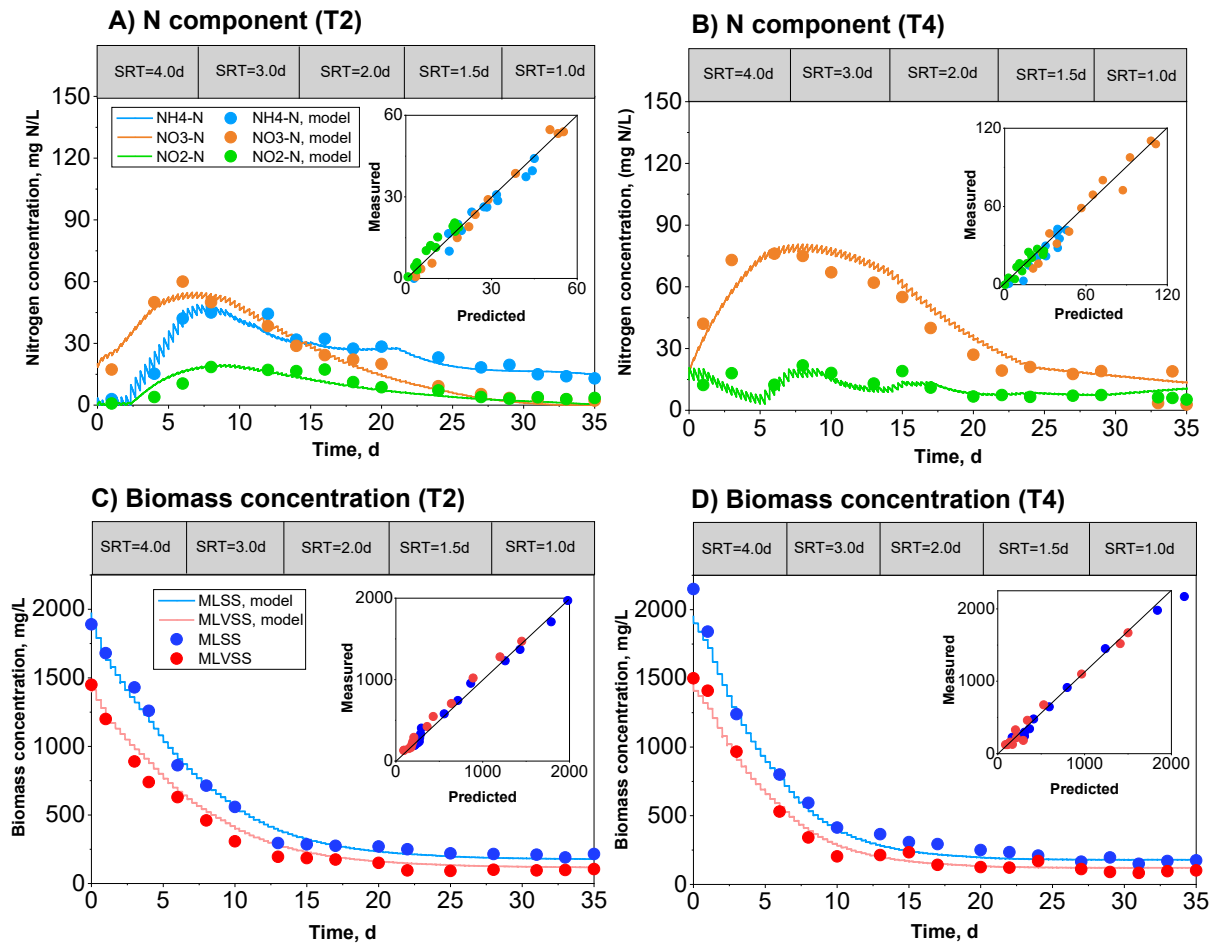
287 **3.3. Model calibration and validation**

288 The experimental observations and predicted behaviors of N species ( $\text{NH}_4^+\text{-N}$ ,  $\text{NO}_3^-\text{-N}$ , and  
289  $\text{NO}_2^-\text{-N}$ ), and biomass concentrations for the calibrated model (trials T1 and T3) are shown in  
290 Figure 4. Similar data for the validated model (trials T2 and T4) are shown in Figure 5. In all the  
291 trials, the biomass concentrations (MLSS, MLVSS) were continuously decreased and stabilized  
292 after two weeks at below 400 mg/L. Moreover, regardless of the substrate ( $\text{NH}_4^+\text{-N}$  vs.  $\text{NO}_2^-\text{-N}$ ),  
293 the behavior of  $\text{NO}_3^-\text{-N}$  was generally similar with a peak concentration occurring after one week.  
294



295  
296 **Figure 4.** Observed data vs. model predictions for the calibrated model: A) N components in trial T1, B) N  
297 components in trial T3, C) Biomass concentrations in trial T1, D) Biomass concentrations in trial T3  
298





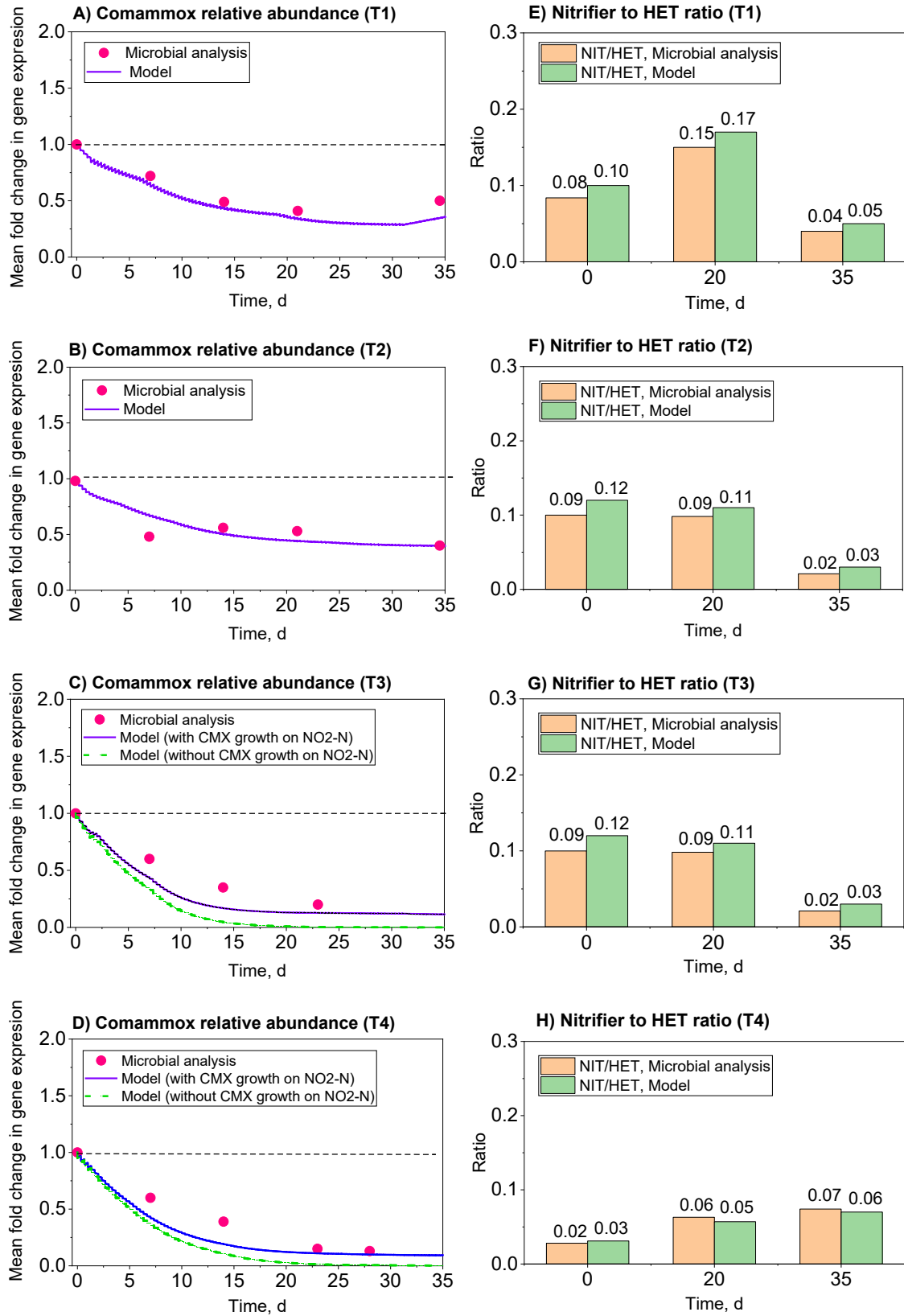
299  
 300 **Figure 5.** Observed data vs. model predictions for the validated model: A) N components in T2, B) N components  
 301 in T4, C) Biomass concentrations in T2, D) Biomass concentrations in T4

302  
 303 In addition to the standard predictions (N species and biomass), the newly developed model also  
 304 predicted two microbiological indicators, including the relative abundance of comammox  
 305 bacteria and nitrifiers (NIT) to heterotrophs (HET) ratio (Figure 6). The relative abundance of  
 306 comammox bacteria in the trials with  $\text{NH}_4^+\text{-N}$  substrate (T1 and T2) decreased and stabilized at  
 307 0.4-0.5 (Figure 6a-b), while in the trials with  $\text{NO}_2^-\text{-N}$  substrate (T3 and T4), the abundance  
 308 sharply decreased in the first week and stabilized at 0.1-0.2 at the end of trials (Figure 6c-d). The  
 309 results with  $\text{NO}_2^-\text{-N}$  substrate strongly suggest that comammox bacteria can grow on  $\text{NO}_2^-\text{-N}$ , as  
 310 the model predictions significantly worsened without considering that process (Figure 6c-d).

311  
312 The NIT/HET ratios in trials T1 and T2 were stable at 0.1-0.15 at the beginning and middle  
313 phases and then decreased to 0.05 at the end of the trials (Figure 6e-f). In contrast, the NIT/HET  
314 ratios in trials T3 and T4 were relatively stable (0.04-0.05) at the beginning and middle phase,  
315 and then increased to >0.05 at the end of the trials (Figure 6g-h).

316  
317 Table 3 shows a list of the model parameters along with their related values and sources of  
318 information. Due to high sensitivity ( $S_{i,j} \geq 0.5$ ), the  $\mu$  and  $K_o$  for all the nitrifier groups (AOB,  
319 NOB1, NOB2, CMX), and  $\mu$  for heterotrophs were adjusted during mathematical optimization.  
320 The estimated values were further discussed in relation to literature data (see Section 4.1). The  
321 extended model prediction performance for each model output ( $\text{NH}_4^+\text{-N}$ ,  $\text{NO}_3^-\text{-N}$ ,  $\text{NO}_2^-\text{-N}$ ) is  
322 presented in Table 4. The calibrated model exposed a high goodness-of-fit for all the outputs in  
323 terms of  $R^2$  (>0.87) and RMSE and MAE errors (2.20-3.4), while the validated model revealed  
324 slightly decreased (<7%)  $R^2$ , and slightly increased (<15%) errors (RMSE, MAE) compared to  
325 the calibration period. The Janus coefficient varied in the range of 1.31-1.97, which also  
326 confirmed the model validity.

327



328  
329  
330

**Figure 6.** Observed vs. predicted relative abundances of comammox bacteria (A-D), and the ratio of nitrifiers to heterotrophs (E-H) for trials T1-T4

331 **Table 3.** List of the adjusted kinetic parameters during model calibration, their values and sources of information

Parameter	Unit	Bacterial group					Source
		AOB	NOB 1 <i>Nitrospira</i>	NOB 2 <i>Nitrobacter</i>	CMX	HET	
<b>Kinetic</b>							
$\mu$	d <sup>-1</sup>	0.38	0.21	0.60	0.20	1.00	Optimization
K <sub>O</sub>	mg O <sub>2</sub> /L	-	-	0.45	0.30	-	Optimization
K <sub>O</sub>	mg O <sub>2</sub> /L	0.17	0.13	-	-	-	Experimental
K <sub>O</sub>	mg O <sub>2</sub> /L	-	-	-	-	0.20 <sup>d</sup>	Literature
K <sub>NH4</sub>	mg NH <sub>4</sub> /L	0.67 <sup>a</sup>	-	-	0.012 <sup>b</sup>	-	Literature
K <sub>NO2</sub>	mg NO <sub>2</sub> /L	-	-	0.76 <sup>a</sup>	6.29 <sup>b</sup>	0.20 <sup>d</sup>	Literature
K <sub>NO2</sub>	mg NO <sub>2</sub> /L	-	0.06	-	-	-	Experimental
K <sub>NO3</sub>	mg NO <sub>2</sub> /L	-	-	-	-	0.20 <sup>d</sup>	Literature
b	d <sup>-1</sup>	0.15 <sup>c</sup>	0.05 <sup>c</sup>	0.05 <sup>c</sup>	0.05 <sup>f</sup>	0.40 <sup>d</sup>	Literature
<b>Stoichiometric</b>							
Y	gCOD/ gN	0.15 <sup>c</sup>	0.05 <sup>c</sup>	0.05 <sup>c</sup>	0.15 <sup>c</sup>	-	Literature
Y <sub>H</sub>	gCOD/gCOD	-	-	-	-	0.6 <sup>d</sup>	Literature

332  $\mu$ : Max. growth rate constant, K<sub>O</sub>: Dissolved oxygen half-saturation constant, K<sub>NH4</sub>: Ammonia half-saturation  
333 constant, K<sub>NO2</sub>: Nitrite half-saturation constant, Y: Yield coefficient, b: Decay rate, a: (Yu et al., 2020), b: (Koch et al  
334 2019), c: (Metcalf and Eddy 2003) d: (Hiatt and Grady, 2008), e: assumed equal to AOB (Roots et al. 2019), f: equal  
335 to NOB (Mehrani et al. 2021)  
336

337

338 **Table 4.** Summarized information on the model efficiency during the calibration and validation periods

Variable	Calibration phase				Validation phase				
	Trials	R <sup>2</sup>	RMSE	MAE	Trials	R <sup>2</sup>	RMSE	MAE	J <sup>2</sup>
NH <sub>4</sub> <sup>+</sup> -N		0.90	2.30	2.42		0.87	2.58	3.11	1.25
NO <sub>3</sub> <sup>-</sup> -N	T 1	0.90	2.38	2.95	T 2	0.86	2.72	3.25	1.30
NO <sub>2</sub> <sup>-</sup> -N		0.86	2.47	3.48		0.81	3.44	3.67	1.93
NH <sub>4</sub> <sup>+</sup> -N		-	-	-		-	-	-	-
NO <sub>3</sub> <sup>-</sup> -N	T 3	0.90	2.32	2.62	T 4	0.84	3.09	3.95	1.77
NO <sub>2</sub> <sup>-</sup> -N		0.88	2.56	2.69		0.80	3.58	4.32	1.95

339

340 **3.4. Contribution of accompanying processes in N conversion**

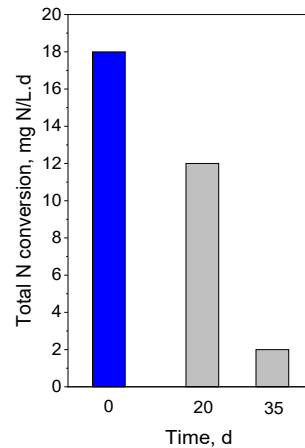
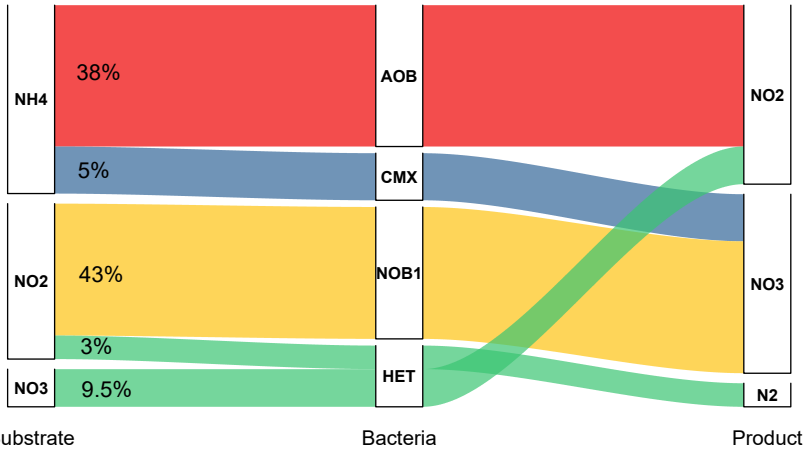
341 Figure 7 shows the N conversion pathways in trial T1 with NH<sub>4</sub><sup>+</sup>-N substrate. The relative  
 342 contributions of some bacteria groups were significantly shifted during the trial. The canonical  
 343 NOB1 and comammox bacteria continuously reduced their abundances - from 43 to 21% (NOB1)  
 344 and from 5% to 1% (comammox). The contribution of NOB2 was negligible (<0.1%). The AOB  
 345 increased their contribution from 38% at the beginning to 50% at the end of the trial. The  
 346 contribution of denitrifying heterotrophs, mediating two steps of denitrification, increased from  
 347 the initial 12.5% to 28% at the end of the trial.

348

349 Figure 8 shows the N conversion pathways in trial T3 with NO<sub>2</sub><sup>-</sup>-N substrate. The contribution of  
 350 NOB1 was substantially decreased from 79% to 7%, while the NOB2 contribution had an  
 351 increasing trend (4% to 89%) in the course of the trial. The comammox bacteria and denitrifying  
 352 heterotrophs decreased their contributions, respectively, from 4% to <1% and from 16% to 3%.

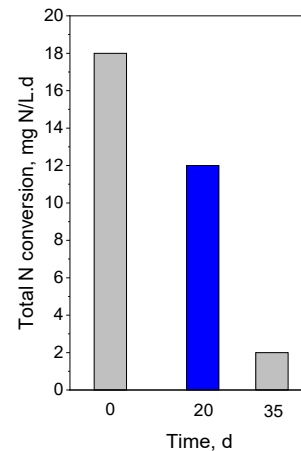
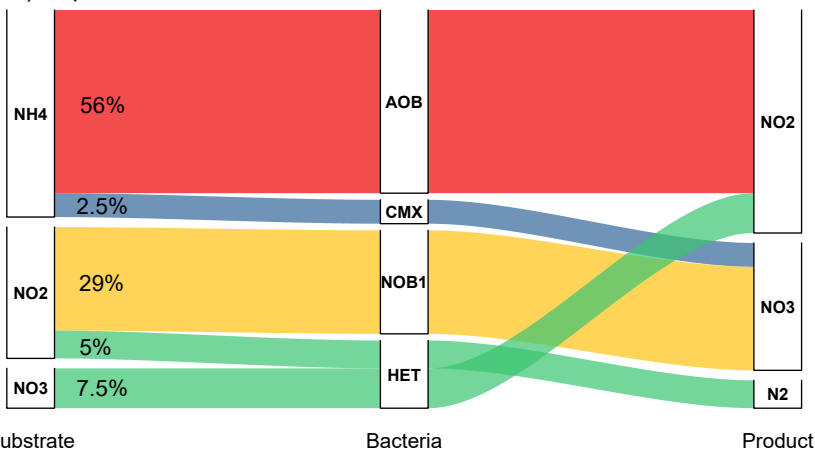
353

A) Experiment T1, T= 0d (beginning)



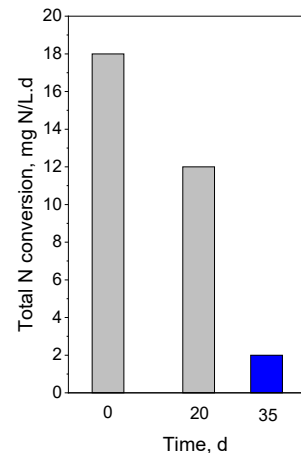
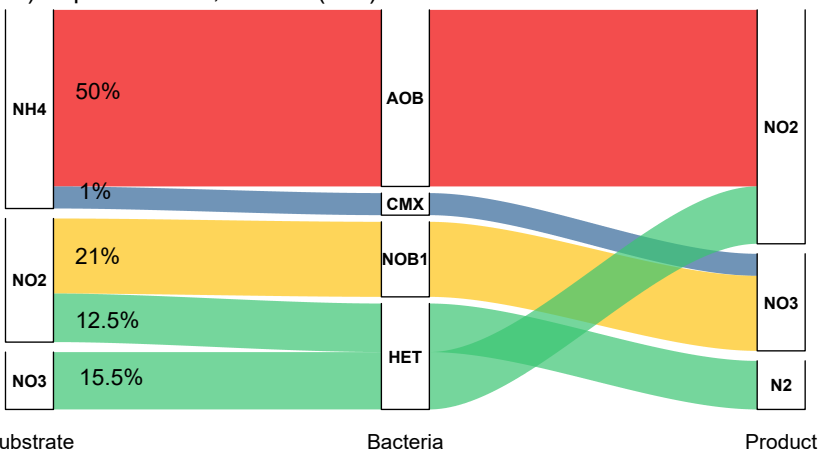
354

B) Experiment T1, T= 20d



355

C) Experiment T1, T= 35d (end)



356

357

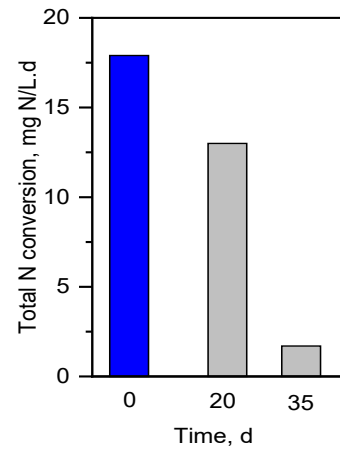
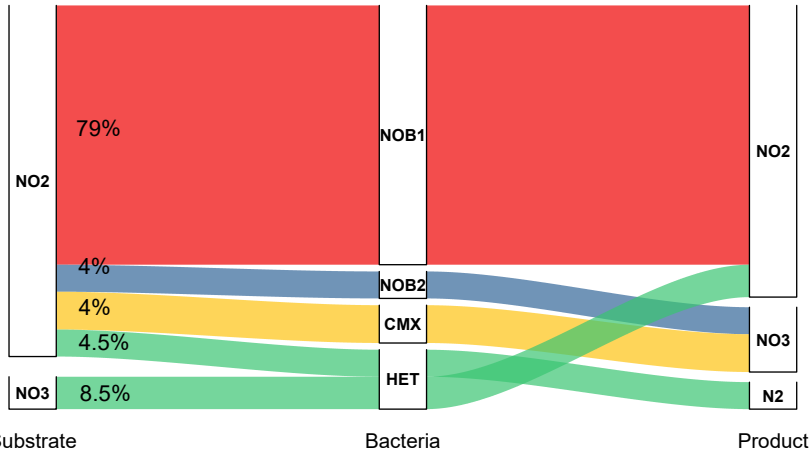
358

359

360

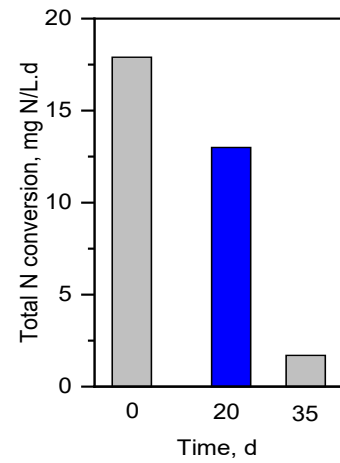
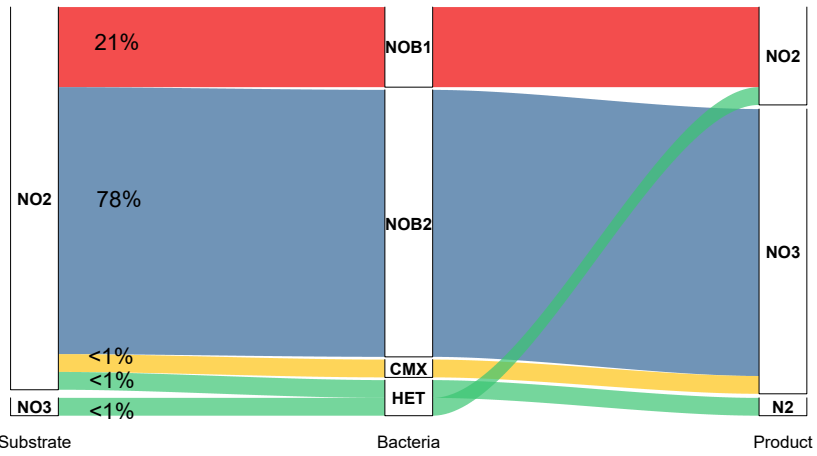
**Figure 7.** Sankey diagram showing the N conversion pathways in trial T1 (% represent the shares in the total conversion rate (mg N/L.d): A) 0 d, B) 20 d, C) 35 d

A) Experiment T3, T= 0d (beginning)



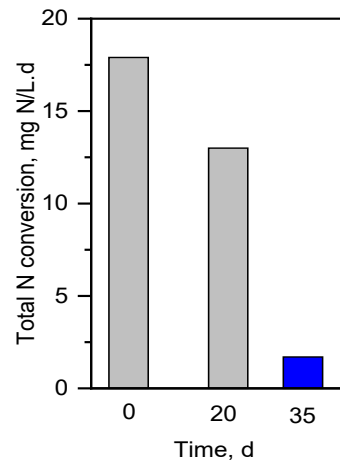
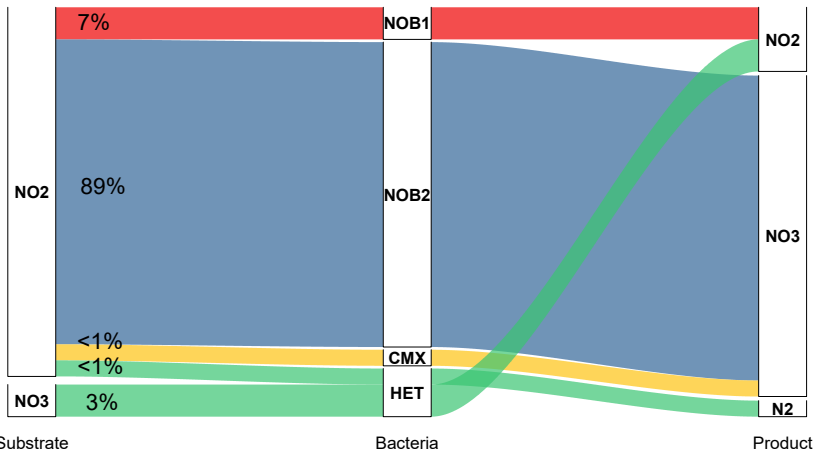
361

B) Experiment T3, T= 20d



362

C) Experiment T3, T= 35d



363

364 **Figure 8.** Conversion pathways of the N species for trial T3 (% represent the shares in the absolute total N  
 365 conversions (mg N/L.d): A) 0 d, B) 20 d, C) 35 d  
 366

367

368 **4. DISCUSSION**

369 **4.1. Factors influencing the competition between *Nitrospira* and *Nitrobacter***

370 In the present study, it has been confirmed that the NOB competition is predominantly impacted  
371 by substrate ( $\text{NO}_2^-$ -N) concentrations, rather than temperature. Blackburne et al. (2007) attributed  
372 the dominance of *Nitrospira* over *Nitrobacter* under low  $\text{NH}_4^+$ -N and  $\text{NO}_2^-$ -N concentrations to  
373 much lower inhibition thresholds of free ammonia (FA) and free nitrous acid (FNA). These  
374 thresholds were respectively 0.04–0.08 mg  $\text{NH}_3$ -N/L and 0.03 mg  $\text{HNO}_2$ -N/L for *Nitrospira*, and  
375 10 mg  $\text{NH}_3$ -N/L and 0.2–0.4 mg  $\text{HNO}_2$ -N/L for *Nitrobacter*.

376  
377 It has been shown in several studies (Huang et al., 2010; Nogueira and Melo, 2006; Park et al.,  
378 2017) that *Nitrobacter* was the dominating NOB at higher  $\text{NO}_2^-$ -N concentrations ( $> 80$  mg N/L),  
379 whereas *Nitrospira* thrived better under lower  $\text{NO}_2^-$ -N conditions. Moreover, Nogueira and Melo  
380 (2006) observed that the dominance of *Nitrobacter* was not reverted after decreasing the  $\text{NO}_2^-$ -N  
381 concentration to the original (low) level. The authors provided two possible explanations for that  
382 observation, including inhibition of *Nitrospira* by high densities of *Nitrobacter* or not sufficient  
383 experimental period.

384  
385 The DO concentration is another important operational factor that influences *Nitrospira*  
386 abundance in WWTPs ( Ushiki et al., 2017; Chang et al., 2019). Park et al. (2017) attributed a  
387 strong enrichment of *Nitrospira* (at the expense of *Nitrobacter*) in a DO- and  $\text{NO}_2^-$ -N -limited  
388 SBR to the lower affinity constants of *Nitrospira* for both substrates (see Table S5). (Liu and  
389 Wang, 2013) found that in addition to low DO concentrations (0.2-0.4 mg  $\text{O}_2$ /L), extending the  
390 SRT from 10 d to 40 d resulted in the dominance of *Nitrospira* over *Nitrobacter*.

391



392 Li et al., (2021) found that the SRT of 10 d and shorter aeration times (1.5 h) allowed to  
393 completely wash out NOB from the system. Gradually prolonged aeration times (3-3.5 h),  
394 applied subsequently, did not result in enriching NOB. Both *Nitrospira* and *Nitrobacter*  
395 abundances remained stable, but at a low level, which resulted in maintaining long-term NO<sub>2</sub><sup>-</sup>-N  
396 accumulation in a wide temperature range (18-29 C).

397  
398 *Nitrospira* may be better adapted to slightly higher pH (8–8.3 vs. 7.6–8.2) and temperatures (29–  
399 30 °C vs. 24–25 °C) in addition to low NO<sub>2</sub><sup>-</sup>-N and DO concentrations. Sun et al., (2022)  
400 investigated the coexistence of *Nitrobacter* and *Nitrospira* at various pH (6.0-8.5). The optimum  
401 pH of 7.0 was found in terms of the maximum specific growth rate ( $\mu$ ) and substrate affinity  
402 ( $K_{NO_2}$ ) for NO<sub>2</sub><sup>-</sup>-N oxidation, which also correlated with the highest absolute abundances of the  
403 functional genes of *Nitrobacter* (*nxrA*) and *Nitrospira* (*nxB*).

404  
405 Ushiki et al. (2017) hypothesized that *Nitrospira* had other characteristics to compete with  
406 *Nitrobacter* and other NOB in nitrite-limited environments. *Nitrobacter* has a cytoplasmic nitrite  
407 oxidoreductase (*nxrA*) that is responsible for the reverse transport of NO<sub>2</sub><sup>-</sup>-N and NO<sub>3</sub><sup>-</sup>-N through  
408 the inner membrane. On the contrary, *Nitrospira* encodes for periplasmic *nxB*, which catalyses  
409 nitratation. The periplasmic oxidation is advantageous since it generates a larger specific proton  
410 motive force and avoids the transmembrane exchange of NO<sub>2</sub><sup>-</sup>-N and NO<sub>3</sub><sup>-</sup>-N (Pester et al.,  
411 2014).

412  
413 Table S5 shows a literature review of the kinetic and stoichiometric parameters for *Nitrospira*  
414 and *Nitrobacter*. The ranges of  $\mu$  for r-strategist *Nitrobacter* and K-strategist *Nitrospira* are 0.31-  
415 1.28 d<sup>-1</sup> and 0.15-0.93 d<sup>-1</sup>, respectively. In the present study, the estimated  $\mu$  for *Nitrobacter* (0.6



416  $d^{-1}$ ) was three times higher than *Nitrospira* ( $0.21 d^{-1}$ ). In addition, the experimentally obtained  $K_o$   
417 of  $0.13 \text{ mgO}_2/\text{L}$  for NOB1 (*Nitrospira*) is slightly lower than the overall ranges in Table S6  
418 ( $K_{O,Nitrobacter} = 0.17\text{-}4.32 \text{ mgO}_2/\text{L}$ ,  $K_{O,Nitrospira} = 0.33\text{-}1.35 \text{ mgO}_2/\text{L}$ ), while the optimized  $K_o$  of  $0.45$   
419  $\text{mgO}_2/\text{L}$  for NOB2 is in the lower range ( $0.45\text{-}1.35 \text{ mgO}_2/\text{L}$ ) reported by Yu et al. (2020). It  
420 should be noted, however, that in the literature (O'Shaughnessy, 2016), the  $K_o$  values for  
421 *Nitrospira* and other NOB genera were as low as  $0.04 d^{-1}$ .

422

#### 423 **4.2. Role of comammox-*Nitrospira* in the systems fed with different N substrates**

424 Maddela et al. (2021) noted that comammox bacteria have several competitive advantages over  
425 coexisting canonical nitrifiers, including the capability of thriving at low DO levels and a high  
426 substrate affinity. The high  $\text{NH}_4^+\text{-N}$  affinity of pure cultured comammox bacteria (*N. inopinata*)  
427 is indicated by extremely low half-saturation constants, which are 4- to 2500-fold lower than the  
428 values reported for AOB. Comammox bacteria also show a lower  $\text{NO}_2^-\text{-N}$  affinity than canonical  
429 NOB. Moreover, the abundances of comammox bacteria (*N. inopinata*) showed significant  
430 positive correlations with canonical NOB rather than AOB, which may suggest that comammox  
431 bacteria more actively mediate  $\text{NO}_2^-\text{-N}$  oxidation rather than  $\text{NH}_4^+\text{-N}$  oxidation. The authors  
432 concluded that switches between the modes of  $\text{NH}_4^+\text{-N}$  and  $\text{NO}_2^-\text{-N}$  oxidation in comammox  
433 bacteria remain unknown, and it is difficult to identify the environmental and operational factors  
434 determining the preferred nitrogen source.

435

436 The simulation results of the present study, strongly support the hypothesis that comammox  
437 bacteria can grow on  $\text{NO}_2^-\text{-N}$ . Following the discovery of comammox, it was thought that  
438 comammox-*Nitrospira*, do not possess this ability (Koch et al., 2019). Based on the findings of a  
439 previous investigation by Kits et al. (2017), this was explained by an extremely low  $\text{NO}_2^-\text{-N}$

440 affinity. In comparison with canonical *Nitrospira*, *N. inopinata* (comammox bacteria) had a 50-  
441 fold lower  $\text{NO}_2^-$ -N affinity (Kits et al., 2017). In a recent study, Shao and Wu (2021) found that  
442 the  $\text{NO}_2^-$ -N affinities were variable among the comammox species. Under  $\text{NH}_4^+$ -N limiting  
443 conditions, some authors did not exclude the possibility of comammox bacteria using  $\text{NO}_2^-$ -N as  
444 electron donors (Kits et al., 2017; Palomo et al., 2018; Roots et al., 2019).

445  
446 There is no consensus in the literature if  $\text{NO}_2^-$ -N is released outside of the cells during the  
447 comammox process. Kits et al. (2017) observed that comammox *Nitrospira* could produce  $\text{NO}_2^-$ -  
448 N as an extracellular transit product during complete nitrification. Transient  $\text{NO}_2^-$ -N  
449 accumulation produced by *N. inopinata* (comammox *Nitrospira*) during nitritation was reported  
450 by Ren et al. (2020). In contrast, Wu et al. (2020) found that comammox *Nitrospira* consumed  
451  $\text{NH}_4^+$ -N and produced  $\text{NO}_3^-$ -N at the ratio of nearly 1:1 without any  $\text{NO}_2^-$ -N accumulation.

#### 452 453 **4.3. Further developments of two-NOB models describing the competition with other NOB** 454 **groups**

455 The model developed in the present study may be used to describe a competition of *Nitrospira*  
456 with NOB genera other than *Nitrobacter*. In particular, *Ca. Nitrotoga* has been detected as the  
457 main NOB genus, either alone or together with *Nitrospira*, in different full-scale WWTPs  
458 worldwide (Lücker et al., 2015; Saunders et al., 2016; Chen et al. 2020), and many pilot-scale  
459 systems (Figdore et al., 2018; Jiang et al., 2018; Persson et al., 2017; Wu et al., 2018; Zheng et  
460 al., 2019b). *Ca. Nitrotoga* can oxidize  $\text{NO}_2^-$ -N at temperatures ranging from 4 to 28°C (Lantz et  
461 al., 2021), its optimum temperature (22-23°C) is lower compared to other NOB genera (Zheng et  
462 al., 2020; Ishii et al., 2020). Nowka et al. (2015) observed that *Ca. Nitrotoga* outcompeted  
463 *Nitrospira* and *Nitrobacter* during a long-term cultivation at 5 and 10°C. Liu et al. (2021)

464 calculated a very low temperature correction factor of 1.042 in the temperature range of 4-22 °C  
465 for NOB dominated by *Ca. Nitrotoga*. Speick et al. (2021) concluded that the adaptation of *Ca.*  
466 *Nitrotoga* to low temperatures may be beneficial for the recovery of nitrification during cold  
467 seasons.

468  
469  $K_O$  for *Ca. Nitrotoga* has been determined by Zheng et al. (2020) as  $0.59 \pm 0.11$  mg O<sub>2</sub>/L. This  
470 value is slightly higher than  $K_O$  for *Nitrospira*, and much lower than *Nitrobacter* (see Table 5).  
471 Both *Nitrospira* and *Ca. Nitrotoga* resisted at intermittent aeration in a PN/A system  
472 (Gustavsson, 2020), whereas in another study, *Ca. Nitrotoga* was shown to have a lower DO  
473 affinity than *Nitrospira* (Zheng et al. 2020). Qian et al. (2021) found in a partial  
474 nitrification/anammox (PN/A) system that increasing the DO concentration from 0.4 to 1.8 mgO<sub>2</sub>/L  
475 led to an increased abundance of *Ca. Nitrotoga* over *Nitrospira*. On the contrary, Jiang et al.  
476 (2018) found that a high DO of 2–2.5 mgO<sub>2</sub>/L was sufficient for the washout of both *Nitrospira*  
477 and *Ca. Nitrotoga* in a PN/A system.

478  
479 Higher substrate concentrations may be beneficial to *Nitrotoga* (Nowka et al. 2015). Kinnunen et  
480 al. (2017) discovered that at a NO<sub>2</sub><sup>-</sup>-N concentration of 1 mg N/L, *Ca. Nitrotoga* outcompeted  
481 *Nitrospira* in a biofilm community, but *Nitrospira* dominated at a tenfold lower substrate  
482 concentration.  $K_{NO_2}$  for *Ca. Nitrotoga* was reported in a wide range of 0.345-1.68 mg N/L (Zheng  
483 et al., 2020; Kitzinger et al. 2018; Ishii et al. 2017; Wegen et al. 2019; Nowka et al. 2015). *Ca.*  
484 *Nitrotoga* was also shown to be much more resistant to free ammonia (FA) and free nitrous acid  
485 (FNA) exposure than *Nitrobacter* and *Nitrospira* (Li et al. 2020, Zheng et al., 2021).

486

487 The pH preference of *Ca. Nitrotoga* is neutral to slightly alkaline range as typical for nearly all  
488 NOB (Spieck et al., 2021). The optimum pH for *Ca. Nitrotoga* has been determined in a wide  
489 range as 7.1 – 7.6 (Kitzinger et al., 2018), 7.5 (Zheng et a., 2020), 8.3 (Ishii et al., 2020).

490

#### 491 **4.4. Interactions of nitrifiers and heterotrophs in N removal systems fed with inorganic** 492 **carbon**

493 In the present study, the strategy of progressive SRT reduction and the lack of organic carbon in  
494 the feed resulted in re-arrangements within the heterotrophic bacteria subpopulation (Table S2).

495 Bacteria belonging to the order *Saprospiraceae* and genera *Caldilinea*, *Curvibacter*, *Dokdonella*,  
496 *Holophaga*, *Tetrasphaera* constituted predominant components in the inoculum biomass.

497 However, during all the trials, those bacteria were systematically outcompeted by members of  
498 *Acidovorax*, *Hydrogenophaga*, *Comamonas*, *Pseudomonas*, *Simplicispira*, and *Thermomonas*.

499

500 Based on the reported characteristics of the identified heterotrophs, there are three possible  
501 mechanisms of the surveillance and competitiveness of those bacteria in comparison with other  
502 heterotrophs under extremely short SRTs and inorganic feeding medium: (i) heterotrophic  
503 denitrification with soluble microbial products (SMP) and extracellular polymeric substances  
504 (EPS), generated by AOB and NOB (Nogueira et al. 2005; Sepehri and Sarrafzadeh 2019), (ii)  
505 heterotrophic nitrification (Chen et al. 2012), (iii) predation of heterotrophs on autotrophic  
506 bacteria (Dolinšek et al. 2013).

507

508 In particular, during the trials with  $\text{NH}_4\text{-N}$  as a sole N source, a wider range and more equally  
509 represented heterotrophic bacteria groups have been detected during the final stages. Similar to  
510 the present study, a noticeable occurrence of the *Acidovorax* and *Pseudomonas* representatives in



511 the reactor fed with an inorganic medium was observed by Keluskar et al. (2013). The growth of  
512 those heterotrophs was supported by organic compounds, such as pyruvate, excreted by AOB  
513 (*Nitrosomonas*). An additional metabolic pathway enabling the survival of specific heterotrophs  
514 (*Hydrogenophaga*) in the systems operated under the limited carbon availability is  
515 hydrogenotrophic denitrification with the utilization of hydrogen in the absence of organic  
516 compounds. Furthermore, representatives of *Rhodococcus* have been characterized as bacteria  
517 which are capable of performing simultaneous heterotrophic nitrification and aerobic  
518 denitrification (Chen et al. 2012).

519  
520 In the present study, in the trials with  $\text{NO}_2\text{-N}$  as a sole N source, members of the *Comamonas*  
521 genera outcompeted other heterotrophs, and their relative abundances exceeded 50% in both trials  
522 (at 12 and 20°C). Representatives of the *Comamonas* are well known denitrifying heterotrophs,  
523 which are capable of utilizing a wide range of organic compounds, such as amino acids,  
524 carboxylic acids, steroids and aromatic compounds (Wu et al., 2018), thus due to wide metabolic  
525 properties were capable to develop substrate dependencies with *Nitrobacter* NOB.

526  
527 Predation is another factor affecting the occurrence of specific heterotrophs and their interaction  
528 with the nitrifiers (Dolinšek et al. 2013). Daims et al. (2016) showed that abundances of  
529 *Nitrospira* were dramatically reduced due to the predation by *B. bacteriovorus*. In the present  
530 study, during the trials with  $\text{NH}_4\text{-N}$ , predator bacteria belonging to the *Bdellovibrio* genus were  
531 detected in the abundances > 3%. On the other hand, lower abundances of these bacteria were  
532 found during the trials with  $\text{NO}_2\text{-N}$ , when *Nitrobacter* was predominant. This finding suggests  
533 that predation may indeed reflect a selective pressure on specific NOB.

534

535 **5. CONCLUSIONS**

- 536     ▪ A two-step nitrification model was extended with different NOB groups (competing r  
537         strategists vs. K strategists) to increase the prediction accuracy of modeling nitrifying systems  
538         under diverse NO<sub>2</sub><sup>-</sup>-N availabilities in the substrate.
- 539     ▪ In addition to the standard prediction parameters (N species and biomass concentrations),  
540         microbiological indicators such as the relative abundance of comammox and the ratio of  
541         nitrifiers to heterotrophs, are useful target variables for calibration of mechanistic models as  
542         they revealed the dominant conversion pathways in the studied systems.
- 543     ▪ A combination of microbiological analyses and modeling simulation results confirmed that  
544         comammox bacteria can grow on NO<sub>2</sub><sup>-</sup>-N as a sole N substrate.
- 545     ▪ In contrast to canonical nitrifiers, comammox played a minor role in the study system.  
546         However, the impact of these bacteria needs to be further explored by modeling systems  
547         containing a higher abundance of *Nitrospira*.
- 548     ▪ Even though comammox played a minor role in the studied system compared to the canonical  
549         nitrifiers, the impact of these bacteria should further be explored by modeling systems  
550         containing a higher abundances of *Nitrospira*.

551

552 **ACKNOWLEDGMENTS**

553 This study was supported by the Polish National Science Center under project no. UMO-  
554 2017/27/B/NZ9/01039.

555

556

557

558 **REFERENCES**

- 559 Al-Hazmi HE, Lu X, Majtacz J, Kowal P, Xie L, Makinia J. Optimization of the Aeration Strategies  
560 in a Deammonification Sequencing Batch Reactor for Efficient Nitrogen Removal and  
561 Mitigation of N<sub>2</sub>O Production. *Environmental Science & Technology* 2021; 55: 1218-1230.
- 562 Blackburne R, Vadivelu VM, Yuan Z, Keller J. Kinetic characterisation of an enriched Nitrospira  
563 culture with comparison to Nitrobacter. *Water Research* 2007; 41: 3033-3042.
- 564 Cao J, Zhang T, Wu Y, Sun Y, Zhang Y, Huang B, et al. Correlations of nitrogen removal and core  
565 functional genera in full-scale wastewater treatment plants: Influences of different  
566 treatment processes and influent characteristics. *Bioresource Technology* 2020; 297:  
567 122455.
- 568 Cao Y, van Loosdrecht MCM, Daigger GT. Mainstream partial nitrification–anammox in municipal  
569 wastewater treatment: status, bottlenecks, and further studies. *Applied Microbiology and  
570 Biotechnology* 2017; 101: 1365-1383.
- 571 Chang M, Wang Y, Pan Y, Zhang K, Lyu L, Wang M, et al. Nitrogen removal from wastewater  
572 via simultaneous nitrification and denitrification using a biological folded non-aerated filter.  
573 *Bioresource Technology* 2019; 289: 121696.
- 574 Chen P, Li J, Li QX, Wang Y, Li S, Ren T, et al. Simultaneous heterotrophic nitrification and  
575 aerobic denitrification by bacterium *Rhodococcus* sp. CPZ24. *Bioresource Technology*  
576 2012; 116: 266-270.
- 577 Chen H, Wang M, Chang S. Disentangling Community Structure of Ecological System in  
578 Activated Sludge: Core Communities, Functionality, and Functional Redundancy.  
579 *Microbial Ecology* 2020; 80: 296-308.
- 580 Daims H, Lücker S, Wagner M. A New Perspective on Microbes Formerly Known as Nitrite-  
581 Oxidizing Bacteria. *Trends in Microbiology* 2016; 24: 699-712.



- 582 Daims H, Lebedeva EV, Pjevac P, Han P, Herbold C, Albertsen M, et al. Complete nitrification by  
583 Nitrospira bacteria. *Nature* 2015; 528: 504.
- 584 Dolinšek J, Lagkouvardos I, Wanek W, Wagner M, Daims H. Interactions of Nitrifying Bacteria  
585 and Heterotrophs: Identification of a Micavibrio-Like Putative Predator of Nitrospira spp.  
586 *Applied and Environmental Microbiology* 2013; 79: 2027-2037.
- 587 Duan H, Ye L, Wang Q, Zheng M, Lu X, Wang Z, et al. Nitrite oxidizing bacteria (NOB) contained  
588 in influent deteriorate mainstream NOB suppression by sidestream inactivation. *Water*  
589 *Research* 2019; 162: 331-338.
- 590 Feng S, Tan CH, Constancias F, Kohli GS, Cohen Y, Rice SA. Predation by *Bdellovibrio*  
591 bacteriovorus significantly reduces viability and alters the microbial community  
592 composition of activated sludge flocs and granules. *FEMS Microbiology Ecology* 2017; 93:  
593 20-28.
- 594 Figdore BA, Stensel HD, Winkler M-KH. Comparison of different aerobic granular sludge types  
595 for activated sludge nitrification bioaugmentation potential. *Bioresource Technology* 2018;  
596 251: 189-196.
- 597 Gustavsson DJI, Suarez C, Wilén B-M, Hermansson M, Persson F. Long-term stability of partial  
598 nitritation-anammox for treatment of municipal wastewater in a moving bed biofilm reactor  
599 pilot system. *Science of The Total Environment* 2020; 714: 136342.
- 600 Hauduc H, Neumann MB, Muschalla D, Gamerith V, Gillot S, Vanrolleghem PA. Efficiency  
601 criteria for environmental model quality assessment: A review and its application to  
602 wastewater treatment. *Environmental Modelling & Software* 2015; 68: 196-204.
- 603 Henze MG, W., Mino, T., van Loosdrecht, M.C.M. Activated sludge models ASM1, ASM2,  
604 ASM2d and ASM3. London, UK: IWA Publishing, 2000.

- 605 Hiatt WC, Grady CPL. An Updated Process Model for Carbon Oxidation, Nitrification, and  
606 Denitrification. *Water Environment Research* 2008; 80: 2145-2156.
- 607 Huang Z, Gedalanga PB, Asvapathanagul P, Olson BH. Influence of physicochemical and  
608 operational parameters on *Nitrobacter* and *Nitrospira* communities in an aerobic activated  
609 sludge bioreactor. *Water Research* 2010; 44: 4351-4358.
- 610 Ishii K, Fujitani H, Sekiguchi Y, Tsuneda S. Physiological and genomic characterization of a new  
611 ‘*Candidatus Nitrotoga*’ isolate. *Environmental Microbiology* 2020; 22: 2365-2382.
- 612 Jiang H, Liu G-h, Ma Y, Xu X, Chen J, Yang Y, et al. A pilot-scale study on start-up and stable  
613 operation of mainstream partial nitrification-anammox biofilter process based on online  
614 pH-DO linkage control. *Chemical Engineering Journal* 2018; 350: 1035-1042.
- 615 Keene NA, Reusser SR, Scarborough MJ, Grooms AL, Seib M, Santo Domingo J, et al. Pilot plant  
616 demonstration of stable and efficient high rate biological nutrient removal with low  
617 dissolved oxygen conditions. *Water Research* 2017; 121: 72-85.
- 618 Keluskar R, Nerurkar A, Desai A. Mutualism between autotrophic ammonia-oxidizing bacteria  
619 (AOB) and heterotrophs present in an ammonia-oxidizing colony. *Archives of*  
620 *Microbiology* 2013; 195: 737-747.
- 621 Kent TR, Sun Y, An Z, Bott CB, Wang Z-W. Mechanistic understanding of the NOB suppression  
622 by free ammonia inhibition in continuous flow aerobic granulation bioreactors.  
623 *Environment International* 2019; 131: 105005.
- 624 Kinnunen M, Gülay A, Albrechtsen H-J, Dechesne A, Smets BF. *Nitrotoga* is selected over  
625 *Nitrospira* in newly assembled biofilm communities from a tap water source community at  
626 increased nitrite loading. *Environmental Microbiology* 2017; 19: 2785-2793.
- 627 Kits KD, Sedlacek CJ, Lebedeva EV, Han P, Bulaev A, Pjevac P, et al. Kinetic analysis of a  
628 complete nitrifier reveals an oligotrophic lifestyle. *Nature* 2017; 549: 269-272.

- 629 Koch H, van Kessel MAHJ, Lücker S. Complete nitrification: insights into the ecophysiology of  
630 comammox *Nitrospira*. *Applied Microbiology and Biotechnology* 2019; 103: 177-189.
- 631 Laanbroek HJ, Bodelier PLE, Gerards S. Oxygen consumption kinetics of *Nitrosomonas europaea*  
632 and *Nitrobacter hamburgensis* grown in mixed continuous cultures at different oxygen  
633 concentrations. *Archives of Microbiology* 1994; 161: 156-162.
- 634 Lantz MA, Boddicker AM, Kain MP, Berg OMC, Wham CD, Mosier AC. Physiology of the  
635 Nitrite-Oxidizing Bacterium Candidatus *Nitrotoga* sp. CP45 Enriched From a Colorado  
636 River. *Frontiers in microbiology* 2021; 12: 709371-709371.
- 637 Lawson CE, Lücker S. Complete ammonia oxidation: an important control on nitrification in  
638 engineered ecosystems? *Current Opinion in Biotechnology* 2018; 50: 158-165.
- 639 Li S, Duan H, Zhang Y, Huang X, Yuan Z, Liu Y, et al. Adaptation of nitrifying community in  
640 activated sludge to free ammonia inhibition and inactivation. *Science of The Total*  
641 *Environment* 2020; 728: 138713.
- 642 Li S, Li J, Yang S, Zhang Q, Li X, Zhang L, et al. Rapid achieving partial nitrification in domestic  
643 wastewater: Controlling aeration time to selectively enrich ammonium oxidizing bacteria  
644 (AOB) after simultaneously eliminating AOB and nitrite oxidizing bacteria (NOB).  
645 *Bioresource Technology* 2021; 328: 124810.
- 646 Liu G, Wang J. Long-Term Low DO Enriches and Shifts Nitrifier Community in Activated Sludge.  
647 *Environmental Science & Technology* 2013; 47: 5109-5117.
- 648 Liu H, Zhu L, Tian X, Yin Y. Seasonal variation of bacterial community in biological aerated filter  
649 for ammonia removal in drinking water treatment. *Water Research* 2017; 123: 668-677.
- 650 Liu X, Huang M, Bao S, Tang W, Fang T. Nitrate removal from low carbon-to-nitrogen ratio  
651 wastewater by combining iron-based chemical reduction and autotrophic denitrification.  
652 *Bioresource Technology* 2020; 301: 122731.

- 653 Liu Y, Li S, Ni G, Duan H, Huang X, Yuan Z, et al. Temperature Variations Shape Niche  
654 Occupation of Nitrotoga-like Bacteria in Activated Sludge. ACS ES&T Water 2021; 1:  
655 167-174.
- 656 Lückner S, Schwarz J, Gruber-Dorninger C, Spieck E, Wagner M, Daims H. Nitrotoga-like bacteria  
657 are previously unrecognized key nitrite oxidizers in full-scale wastewater treatment plants.  
658 The ISME Journal 2015; 9: 708-720.
- 659 Ma Y, Domingo-Félez C, Plósz BG, Smets BF. Intermittent Aeration Suppresses Nitrite-Oxidizing  
660 Bacteria in Membrane-Aerated Biofilms: A Model-Based Explanation. Environmental  
661 Science & Technology 2017; 51: 6146-6155.
- 662 Maddela NR, Gan Z, Meng Y, Fan F, Meng F. Occurrence and Roles of Comammox Bacteria in  
663 Water and Wastewater Treatment Systems: A Critical Review. Engineering 2021; 0-
- 664 Mehrani M-J, Lu X, Sobotka D, Kowal P, Makinia J. Incorporation of the complete ammonia  
665 oxidation (comammox) process for nitrification modeling in activated sludge systems.  
666 Journal of Environmental Management 2021; 297: 113223.
- 667 Mehrani M-J, Sobotka D, Kowal P, Ciesielski S, Makinia J. The occurrence and role of Nitrospira  
668 in nitrogen removal systems. Bioresource Technology 2020; 303: 122936.
- 669 Mehrani M-J, Sobotka D, Kowal P, Guo J, Makinia J. New insights into modeling two-step  
670 nitrification in activated sludge systems – the effects of initial biomass concentrations,  
671 comammox and heterotrophic activities. Science of the Total Environment 2022, 157628.
- 672 Metcalf and Eddy, Inc., Wastewater Engineering: Treatment and Resource Recovery, 5th Edition.  
673 McGraw-Hill , New York, United States, 2014.
- 674 Metcalf and Eddy, Inc., Wastewater Engineering : Treatment and Reuse, 4th Edition. McGraw-  
675 Hill, New York, United States, 2003.

- 676 Metcalf and Eddy, Inc., Wastewater Engineering: Treatment, Disposal, and Reuse, 3rd Edition.  
677 McGraw-Hill, New York, United States, 1990.
- 678 Nogueira R, Melo LF. Competition between *Nitrospira* spp. and *Nitrobacter* spp. in nitrite-  
679 oxidizing bioreactors. *Biotechnology and Bioengineering* 2006; 95: 169-175.
- 680 Nogueira R, Elenter D, Brito A, Melo LF, Wagner M, Morgenroth E. Evaluating heterotrophic  
681 growth in a nitrifying biofilm reactor using fluorescence in situ hybridization and  
682 mathematical modeling. *Water Science and Technology* 2005; 52: 135-141.
- 683 Nowka B, Daims H, Spieck E. Comparison of Oxidation Kinetics of Nitrite-Oxidizing Bacteria:  
684 Nitrite Availability as a Key Factor in Niche Differentiation. *Applied and Environmental*  
685 *Microbiology* 2015; 81: 745.
- 686 O'Shaughnessy M. Mainstream Deammonification (WERF Report INFR6R11). Water  
687 Environment Research Foundation, 2016, Alexandria, VA (USA).
- 688 Palomo A, Pedersen AG, Fowler SJ, Dechesne A, Sicheritz-Pontén T, Smets BF. Comparative  
689 genomics sheds light on niche differentiation and the evolutionary history of comammox  
690 *Nitrospira*. *Isme j* 2018; 12: 1779-1793.
- 691 Park M-R, Park H, Chandran K. Molecular and Kinetic Characterization of Planktonic *Nitrospira*  
692 spp. Selectively Enriched from Activated Sludge. *Environmental Science & Technology*  
693 2017; 51: 2720-2728.
- 694 Pérez J, Lotti T, Kleerebezem R, Picioreanu C, van Loosdrecht MCM. Outcompeting nitrite-  
695 oxidizing bacteria in single-stage nitrogen removal in sewage treatment plants: A model-  
696 based study. *Water Research* 2014; 66: 208-218.
- 697 Persson F, Suarez C, Hermansson M, Plaza E, Sultana R, Wilén B-M. Community structure of  
698 partial nitrification-anammox biofilms at decreasing substrate concentrations and low  
699 temperature. *Microbial Biotechnology* 2017; 10: 761-772.

- 700 Qian F, Huang Z, Liu Y, Grace OOw, Wang J, Shi G. Conversion of full nitrification to partial  
701 nitrification/anammox in a continuous granular reactor for low-strength ammonium  
702 wastewater treatment at 20 °C. *Biodegradation* 2021; 32: 87-98.
- 703 Regmi P, Miller MW, Holgate B, Bunce R, Park H, Chandran K, et al. Control of aeration, aerobic  
704 SRT and COD input for mainstream nitrification/denitrification. *Water Research* 2014; 57:  
705 162-171.
- 706 Roots P, Wang Y, Rosenthal AF, Griffin JS, Sabba F, Petrovich M, et al. Comammox *Nitrospira*  
707 are the dominant ammonia oxidizers in a mainstream low dissolved oxygen nitrification  
708 reactor. *Water Research* 2019; 157: 396-405.
- 709 Sakoula D, Koch H, Frank J, Jetten MSM, van Kessel MAHJ, Lücker S. Enrichment and  
710 physiological characterization of a novel comammox *Nitrospira* indicates ammonium  
711 inhibition of complete nitrification. *The ISME Journal* 2021; 15: 1010-1024.
- 712 Saunders AM, Albertsen M, Vollertsen J, Nielsen PH. The activated sludge ecosystem contains a  
713 core community of abundant organisms. *The ISME Journal* 2016; 10: 11-20.
- 714 Sepehri A, Sarrafzadeh M-H. Activity enhancement of ammonia-oxidizing bacteria and nitrite-  
715 oxidizing bacteria in activated sludge process: metabolite reduction and CO<sub>2</sub> mitigation  
716 intensification process. *Applied Water Science* 2019; 9: 131.
- 717 Shao Y-H, Wu J-H. Comammox *Nitrospira* Species Dominate in an Efficient Partial Nitrification–  
718 Anammox Bioreactor for Treating Ammonium at Low Loadings. *Environmental Science*  
719 & Technology 2021; 55: 2087-2098.
- 720 Spieck E, Wegen S, Keuter S. Relevance of *Candidatus Nitrotoga* for nitrite oxidation in technical  
721 nitrogen removal systems. *Applied Microbiology and Biotechnology* 2021; 105: 7123-7139.



- 722 Sun H, Zhang H, Zhang F, Yang H, Lu J, Ge S, et al. Response of substrate kinetics and biological  
723 mechanisms to various pH constrains for cultured Nitrobacter and Nitrospira in nitrifying  
724 bioreactor. *Journal of Environmental Management* 2022; 307: 114499.
- 725 Ushiki N, Jinno M, Fujitani H, Suenaga T, Terada A, Tsuneda S. Nitrite oxidation kinetics of two  
726 Nitrospira strains: The quest for competition and ecological niche differentiation. *Journal*  
727 *of Bioscience and Bioengineering* 2017; 123: 581-589.
- 728 Vadivelu VM, Yuan Z, Fux C, Keller J. Stoichiometric and kinetic characterisation of Nitrobacter  
729 in mixed culture by decoupling the growth and energy generation processes. *Biotechnology*  
730 *and Bioengineering* 2006; 94: 1176-1188.
- 731 van Kessel MAHJ, Speth DR, Albertsen M, Nielsen PH, Op den Camp HJM, Kartal B, et al.  
732 Complete nitrification by a single microorganism. *Nature* 2015; 528: 555.
- 733 Wegen S, Nowka B, Spieck E. Low Temperature and Neutral pH Define "Candidatus Nitrotoga  
734 sp." as a Competitive Nitrite Oxidizer in Coculture with Nitrospira defluvii. *Appl Environ*  
735 *Microbiol* 2019; 85.
- 736 Winkler MKH, Boets P, Hahne B, Goethals P, Volcke EIP. Effect of the dilution rate on microbial  
737 competition: r-strategist can win over k-strategist at low substrate concentration. *PLOS*  
738 *ONE* 2017; 12: e0172785.
- 739 Wu L, Ning D, Zhang B, Li Y, Zhang P, Shan X, et al. Global diversity and biogeography of  
740 bacterial communities in wastewater treatment plants. *Nature Microbiology* 2019; 4: 1183-  
741 1195.
- 742 Wu L, Li Z, Zhao C, Liang D, Peng Y. A novel partial-denitrification strategy for post-anammox  
743 to effectively remove nitrogen from landfill leachate. *Science of The Total Environment*  
744 2018; 633: 745-751.

- 745 Yin Q, Sun Y, Li B, Feng Z, Wu G, The r/K selection theory and its application in biological  
746 wastewater treatment processes. *Science of the Total Environment* 2022; 824: 153836
- 747 Yu L, Chen S, Chen W, Wu J. Experimental investigation and mathematical modeling of the  
748 competition among the fast-growing “r-strategists” and the slow-growing “K-strategists”  
749 ammonium-oxidizing bacteria and nitrite-oxidizing bacteria in nitrification. *Science of The*  
750 *Total Environment* 2020; 702: 135049.
- 751 Zaborowska E, Lu X, Małania J. Strategies for mitigating nitrous oxide production and decreasing  
752 the carbon footprint of a full-scale combined nitrogen and phosphorus removal activated  
753 sludge system. *Water Research* 2019; 162: 53-63.
- 754 Zheng M, Li S, Ni G, Xia J, Hu S, Yuan Z, et al. Critical Factors Facilitating Candidatus Nitrotoxa  
755 To Be Prevalent Nitrite-Oxidizing Bacteria in Activated Sludge. *Environmental Science &*  
756 *Technology* 2020; 54: 15414-15423.
- 757 Zheng M, Li S, Dong Q, Huang X, Liu Y. Effect of blending landfill leachate with activated sludge  
758 on the domestic wastewater treatment process. *Environmental Science: Water Research &*  
759 *Technology* 2019a; 5: 268-276.
- 760 Zheng Z, Huang S, Bian W, Liang D, Wang X, Zhang K, et al. Enhanced nitrogen removal of the  
761 simultaneous partial nitrification, anammox and denitrification (SNAD) biofilm reactor for  
762 treating mainstream wastewater under low dissolved oxygen (DO) concentration.  
763 *Bioresource Technology* 2019b; 283: 213-220.
- 764 Zhu A, Guo J, Ni B-J, Wang S, Yang Q, Peng Y. A Novel Protocol for Model Calibration in  
765 Biological Wastewater Treatment. *Scientific Reports* 2015; 5: 8493.
- 766
- 767





768 **Supplementary Information**  
769 *The coexistence and competition of canonical and comammox nitrite oxidizing*  
770 *bacteria in a nitrifying activated sludge system – experimental observations and*  
771 *simulation studies*

772

773 **Mohamad-Javad Mehrani<sup>1</sup>, Przemyslaw Kowal<sup>1</sup>, Dominika Sobotka<sup>1</sup>, Martyna Godzieba<sup>2</sup>, Sławomir**  
774 **Ciesielski<sup>2</sup>, Jianhua Guo<sup>3</sup>, Jacek Makinia<sup>1\*</sup>**

775 <sup>1</sup> Faculty of Civil and Environmental Engineering, Gdansk University of Technology, Narutowicza Street 11/12, 80-233 Gdansk,  
776 Poland

777 <sup>2</sup> Department of Environmental Biotechnology, Department of Environmental Biotechnology, University of Warmia and Mazury  
778 in Olsztyn, Sloneczna 45G, 10-719 Olsztyn, Poland

779 <sup>3</sup>Australian Centre for Water and Environmental Biotechnology (ACWEB, formerly AWMC), The University of Queensland, St.  
780 Lucia, Queensland 4072, Australia

781 \*Correspondence: Jacek Makinia (Email: [jmakinia@pg.edu.pl](mailto:jmakinia@pg.edu.pl), Tel: +48 58 347 19 54, Address: Gdansk University of  
782 Technology, ul. Narutowicza 11/12, 80-233, Gdansk, Poland)

783

784 **S1. Synthetic medium used for the long-term experiments and Influent substrate**

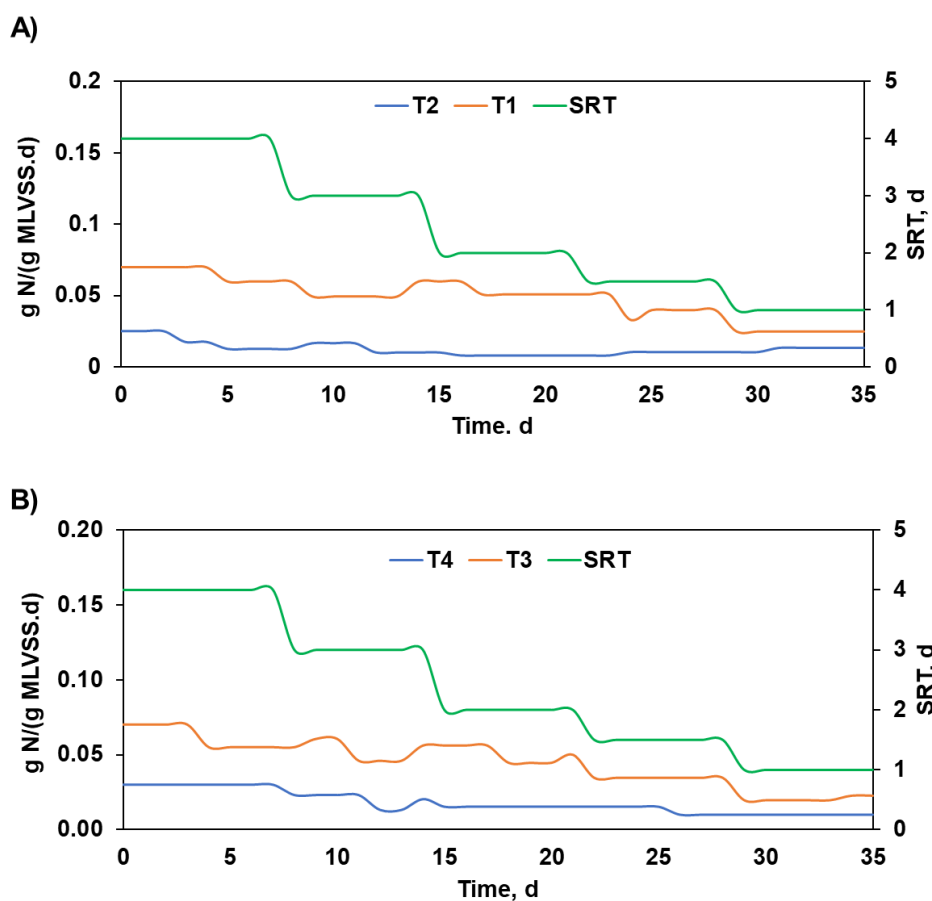
785 **concentrations**

786 **Table S1.** Characteristics of the synthetic medium (NH<sub>4</sub>-N vs. NO<sub>2</sub>-N substrate) used for the long-term washout  
787 experiments

Substrate	Main elements		Tracer solution*	
	Compound	Concentration mg/L	Compound	Concentration g/L
<b>NH<sub>4</sub>-N</b>	NH <sub>4</sub> CL	762	ZnSO <sub>4</sub> ·7H <sub>2</sub> O	0.43
	KHCO <sub>3</sub>	1512	(NH <sub>4</sub> ) <sub>6</sub> Mo <sub>7</sub> O <sub>24</sub> ·4H <sub>2</sub> O	0.22
	CaCl <sub>2</sub>	141	CuSO <sub>4</sub> ·5H <sub>2</sub> O	0.25
	KH <sub>2</sub> PO <sub>4</sub>	50	MnCl <sub>2</sub> ·4H <sub>2</sub> O	0.99
	MgSO <sub>4</sub>	58.6	CoCl <sub>2</sub> ·6H <sub>2</sub> O	0.24
	FeSO <sub>4</sub> ·7H <sub>2</sub> O	9.1	NaWO <sub>4</sub> ·2H <sub>2</sub> O	0.005
	EDTA	6.3	EDTA	15
	Tracer solution*	1	NiCl <sub>2</sub> ·6H <sub>2</sub> O	0.2
			NaSeO <sub>4</sub> ·10H <sub>2</sub> O	0.2
			H <sub>3</sub> BO <sub>3</sub>	0.014
<b>NO<sub>2</sub>-N</b>	NO <sub>2</sub> <sup>-</sup>	172 - 1470	ZnSO <sub>4</sub> ·7H <sub>2</sub> O	0.43
	KHCO <sub>3</sub>	1512	(NH <sub>4</sub> ) <sub>6</sub> Mo <sub>7</sub> O <sub>24</sub> ·4H <sub>2</sub> O	0.22
	CaCl <sub>2</sub>	141	CuSO <sub>4</sub> ·5H <sub>2</sub> O	0.25
	KH <sub>2</sub> PO <sub>4</sub>	50	MnCl <sub>2</sub> ·4H <sub>2</sub> O	0.99
	MgSO <sub>4</sub>	58.6	CoCl <sub>2</sub> ·6H <sub>2</sub> O	0.24
	FeSO <sub>4</sub> ·7H <sub>2</sub> O	9.1	NaWO <sub>4</sub> ·2H <sub>2</sub> O	0.005
	EDTA	6.3	EDTA	15
	Tracer solution*	1	NiCl <sub>2</sub> ·6H <sub>2</sub> O	0.2
			NaSeO <sub>4</sub> ·10H <sub>2</sub> O	0.2
			H <sub>3</sub> BO <sub>3</sub>	0.014

788





790  
 791 **Figure S1-** SRT and influent N loading rate for A) NH<sub>4</sub><sup>+</sup>-N substrate experiments (T1, T2), and B) NO<sub>2</sub><sup>-</sup>-N substrate  
 792 experiments (T3, T4)

793

## 794 S2. Microbiological analytical methods

### 795 S.2.1. DNA extraction

796 Biomass samples for microbial analysis were collected from the SBRs three times: at the beginning  
 797 (inoculum), during the middle phase (25th day), and at the of the experiment (35th day). The

798 biomass samples from the initial experimental stages were transferred to the 50 ml Falcon type  
 799 tubes for sedimentation and thickening. The biomass samples withdrawn during the terminal stages,

800 were separated from the outflows from the experimental SBR by filtration trough through 0.22 μm

801 pore size filters. Each sample was collected in duplicate. Both types of the samples (thickened

802 sludge and biomass deposited on filters) were stored at -25°C prior to DNA extraction. The

803 extraction of the DNA from the biomass samples (100 mg of the thickened sludge or filter slices  
804 with deposited biomass) was carried out using the FastDNA™ SPIN KIT (MP Biomedicals, USA)  
805 following the manufacturer's manual. The DNA acquired from purification was subsequently used  
806 for the Illumina Next Generation Sequencing protocol.

807

### 808 *S.2.2. High-throughput 16S rDNA sequencing*

809 High-throughput Illumina sequencing targeting the V3-V4 region of the 16S rRNA gene was  
810 performed with S-d-Bact-0341-b-S-17 and S-d-Bact-0785-a-A-21 primers (Klindworth et al., 2012)  
811 and NEBNext®High-Fidelity 2X PCR Master Mix (Bio Labs inc., USA) following the  
812 manufacturer's manual. The sequencing reactions were carried out with MiSeq sequencer (Illumina,  
813 USA) by applying the paired-end technology, 2×250 nt with MiSeq Reagent Kit V2 following the  
814 manufacturer's protocols. The obtained raw DNA sequence reads were subjected to quality control  
815 (QC) using the tools available at Usegalaxy server (usegalaxy.org). Paired-end reads were initially  
816 combined with the fastq-join algorithm. The reads were subsequently trimmed and filtered in terms  
817 of the length ( $\geq 400$  bp) and quality (Phred score  $\geq 20$ ) with Filter FASTQ algorithm. The reads  
818 quality at each QC step was validated with FastQC software  
819 ([www.bioinformatics.babraham.ac.uk/projects/fastqc](http://www.bioinformatics.babraham.ac.uk/projects/fastqc)).

820

821 Chimera presence was verified with a chimera check on-line tool powered by UCHIME  
822 (<http://pyro.cme.msu.edu>). The classification of the reads on each taxonomical level was carried  
823 out with the SILVA server ([www.arb-silva.de](http://www.arb-silva.de)) using the database release version 132 at the  
824 similarity level of 90% and operational taxonomic units (OTUs) clustering at 97%. The output data  
825 from the Usegalaxy server were saved into FASTA format and uploaded to the MetaGenome Rapid

826 Annotation Subsystems Technology (MG-RAST) (Meyer et al., 2008) to enable public access to  
827 the files under the accession numbers ranging from mgm4899014.3 to mgm4899025.3.

828

### 829 ***S.2.3 Absolute quantification of the Comammox bacteria by qPCR***

830 Absolute quantification of the comammox amoA genes was performed with primers sets comaA-  
831 244F & comaA-659R and comaB-244F & comaB-659R in order detect and enumerate comammox  
832 *Nitrospira* clades A and B, respectively, in accordance with the protocol proposed by (Pjevac et  
833 al., 2017). The real-time PCR reactions were performed on ABI 7500 real-time PCR thermocycler  
834 (Applied Biosystems) in MicroAmp™ Optical 96-well reaction plates (Applied Biosystems).  
835 Each sample was analysed in triplicate.

836

837 **Table S2.** Composition of the overall bacterial community and dynamics of the most abundant HET bacteria during  
 838 particular experimental trials. The relative abundances are presented in the form of the heatmap in accordance to the  
 839 presented pattern presented pattern

Experimental series (day of the experiment)	NO <sub>2</sub> -N only; 12°C			NO <sub>2</sub> -N only; 20°C			NH <sub>4</sub> -N only; 12°C			NH <sub>4</sub> -N only; 20°C		
	T1			T2			T3			T4		
	1	15	28	1	14	30	1	21	35	1	21	35
BLAST assignment (at >85% similarity)												
uncultured member of Saprospiraceae (HET)	7.1%	3.7%	0.1%	7.6%	3.4%	0.0%	4.16%	1.52%	0.43%	7.26%	0.08%	0.69%
<i>Curvibacter</i> (DEN)	7.5%	1.9%	0.1%	3.7%	0.9%	0.0%	0.0%	0.2%	0.0%	0.2%	0.2%	0.1%
<i>Tetrasphaera</i> (DPAO)	3.5%	2.8%	0.0%	4.8%	2.1%	0.0%	3.7%	0.6%	0.1%	3.0%	0.0%	0.2%
<i>Candidatus</i> Saccharibacteria (DEN)	1.8%	1.3%	0.0%	1.0%	0.5%	0.1%	5.5%	1.8%	0.5%	4.5%	1.3%	0.3%
<i>Dokdonella</i> (DEN)	4.5%	3.6%	0.5%	1.9%	3.3%	0.1%	1.5%	1.3%	1.0%	2.3%	0.7%	4.9%
<i>Gemmatimonas</i> (DPAO)	1.2%	0.9%	0.1%	1.3%	1.4%	0.0%	1.5%	1.1%	0.3%	1.8%	0.0%	1.3%
<i>Holophaga</i> (HET)	2.2%	2.0%	0.1%	0.9%	1.0%	0.0%	2.4%	0.8%	0.2%	3.1%	0.0%	0.5%
<i>Thermomonas</i> (DEN)	4.3%	0.9%	1.0%	3.5%	2.5%	0.1%	0.3%	2.2%	2.7%	0.8%	3.7%	3.1%
<i>Candidatus</i> Microthrix (DPAO)	2.4%	0.8%	0.1%	3.0%	1.8%	0.0%	2.5%	0.5%	0.1%	1.4%	0.0%	0.1%
<i>Acidovorax</i> (DEN)	4.7%	7.9%	2.7%	8.0%	16.2%	1.1%	1.6%	11.3%	12.6%	1.4%	2.7%	3.2%
<i>Terrimonas</i> (HET)	2.1%	1.6%	0.2%	2.4%	1.5%	0.1%	1.0%	0.7%	0.6%	0.9%	0.2%	1.1%
<i>Caldilinea</i> (HET/DEN)	2.4%	2.5%	0.1%	1.7%	2.5%	0.1%	5.8%	1.6%	0.4%	4.8%	0.2%	1.0%
<i>Pelomonas</i> (DEN)	1.0%	6.8%	1.6%	0.9%	16.0%	0.9%	0.8%	1.9%	1.7%	0.5%	2.0%	1.1%
<i>Hyphomicrobium</i> (DEN)	1.6%	0.5%	0.0%	0.5%	0.4%	0.0%	1.5%	0.4%	0.2%	0.8%	0.2%	0.1%
<i>Candidatus</i> Competibacter (GAO)	0.3%	0.6%	0.0%	0.2%	0.2%	0.0%	1.9%	0.8%	0.1%	1.6%	0.0%	0.1%
<i>Asprobacter</i> (HET)	1.3%	0.6%	0.2%	1.0%	0.7%	0.1%	0.2%	0.1%	0.3%	0.2%	0.3%	0.1%
<i>Ferruginibacter</i> (HET)	1.0%	0.7%	0.0%	1.2%	1.0%	0.0%	0.6%	0.3%	0.3%	0.5%	0.2%	1.3%
<i>Dechloromonas</i> (DPAO)	0.3%	0.2%	0.0%	0.8%	0.3%	0.0%	0.2%	0.5%	0.1%	0.0%	0.0%	0.1%
<i>Denitratisoma</i> (DEN)	0.2%	0.1%	0.0%	0.1%	0.1%	0.0%	0.2%	0.1%	0.1%	0.1%	0.0%	0.2%
<i>Thauera</i> (DEN)	0.7%	0.2%	0.2%	1.2%	0.2%	0.0%	2.5%	0.2%	0.0%	1.7%	0.0%	1.6%
<i>Hydrogenophaga</i> (DEN)	0.1%	0.4%	3.6%	0.4%	4.2%	0.7%	0.0%	5.0%	7.6%	0.0%	5.1%	5.1%
<i>Zoogloea</i> (DEN and NIT)	0.0%	0.0%	0.2%	0.2%	0.0%	0.0%	0.0%	0.4%	1.2%	0.1%	0.2%	0.2%
<i>Mycolicibacter</i> (HET)	0.2%	0.2%	4.6%	0.1%	0.1%	3.2%	0.6%	0.2%	0.3%	0.4%	0.4%	0.1%
<i>Comamonas</i> (HET/DEN???)	0.4%	10.9%	48.6%	0.5%	4.1%	77.7%	0.0%	11.2%	6.5%	0.1%	16.7%	6.9%
<i>Legionella</i> (HET)	0.1%	0.1%	3.9%	0.3%	0.2%	0.5%	0.1%	0.0%	0.1%	0.1%	0.6%	0.0%
<i>Simplicispira</i> (DEN)	0.0%	3.7%	4.1%	0.1%	1.0%	0.0%	0.0%	5.0%	4.9%	0.0%	1.5%	2.5%
<i>Pseudoxanthomonas</i> (DEN/new DPAO???)	0.0%	0.0%	0.7%	0.0%	0.1%	0.2%	0.0%	0.9%	4.9%	0.0%	4.0%	0.5%
<i>Rhodoferax</i> (DEN)	7.5%	1.9%	0.1%	3.7%	0.9%	0.0%	0.0%	0.2%	0.0%	0.2%	0.2%	0.1%
<i>Rhodococcus</i> (HET DEN and NIT)	0.0%	0.1%	0.3%	0.0%	0.1%	0.4%	0.0%	0.6%	4.5%	0.0%	13.7%	8.7%
<i>Rhodobacter</i> (DEN)	0.7%	1.1%	0.6%	1.1%	1.0%	0.1%	1.2%	0.5%	0.6%	0.8%	0.1%	0.1%
<i>Sphingopyxis</i> (HET)	0.0%	0.0%	0.3%	0.0%	0.1%	0.2%	0.0%	1.3%	1.4%	0.0%	0.8%	0.6%
<i>Pseudomonas</i> (DEN)	0.0%	1.7%	0.4%	0.2%	2.6%	0.0%	0.0%	0.6%	2.7%	0.0%	14.9%	3.6%
<i>Brevundimonas</i> (DEN)	0.3%	0.2%	0.4%	0.1%	0.9%	0.1%	0.1%	0.6%	1.4%	0.0%	0.6%	1.9%
<i>Denitratimonas</i> (DEN)	1.1%	0.6%	0.2%	2.4%	1.0%	0.0%	0.0%	0.1%	0.2%	0.1%	0.5%	0.9%
<i>Chryseolinea</i> related (HET)	0.8%	0.8%	0.0%	1.0%	1.2%	0.0%	0.8%	2.4%	3.7%	0.5%	0.2%	0.3%
<i>Simplicispira</i> (DEN)	0.0%	3.7%	4.1%	0.1%	1.0%	0.0%	0.0%	5.0%	4.9%	0.0%	1.5%	2.5%
<i>Bdellovibrio</i> (DEN predator)	0.4%	0.2%	0.2%	0.4%	0.5%	0.0%	0.3%	0.5%	0.3%	0.3%	0.4%	3.3%
<i>Ferruginibacter</i> (DEN)	1.0%	0.7%	0.0%	1.2%	1.0%	0.0%	0.6%	0.3%	0.3%	0.5%	0.2%	1.3%
<i>Glutamicibacter</i> (HET)	0.0%	0.0%	0.0%	0.0%	0.0%	0.0%	0.0%	0.0%	0.0%	0.5%	0.2%	1.3%

<i>Flavobacterium (DEN)</i>	0.2%	0.2%	0.1%	0.5%	0.3%	0.1%	0.2%	0.4%	2.3%	0.3%	0.3%	3.1%
<i>TOTAL:</i>	62.9%	66.3%	79.6%	58.0%	76.3%	86.3%	41.8%	63.3%	69.5%	40.7%	63.9%	73.7%

840

841 **S3. Initial biomass concentrations for simulation of the long-term experiments**842 **Table S3.** Initial biomass concentrations for simulation of the long-term experiments

Parameters	Units	Initial biomass concentration			
		T1	T2	T3	T4
$X_{AOB}$	mg COD/L	36.4	34.3	0	0
$X_{NOB1}$	mg COD/L	13	12.5	11.5	11
$X_{NOB2}$	mg COD/L	0.13	0.12	0.11	0.11
$X_{CMX}$	mg COD/L	4.8	6.0	4.5	4.0
$X_{HET}$	mg COD/L	380	405	385	390

843

844



845 **S4. Review on stoichiometric and kinetic parameters**

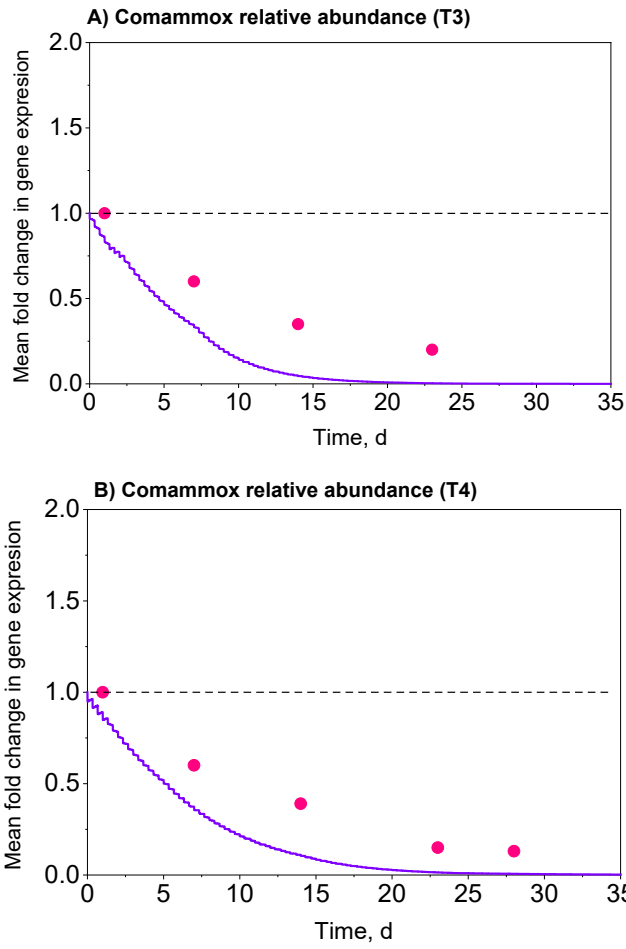
846 **Table S4.** Review of recent literature data on the stoichiometric and kinetic parameters related to the specific groups  
 847 of canonical AOB (r-AOB vs. K-AOB), canonical NOB (r-NOB vs. K-NOB), and comammox bacteria

Parameters (Unit)	Canonical r-AOB ( <i>Nitrosomonas</i> )	Canonical K-AOB ( <i>Nitrospira</i> )	Canonical r-NOB ( <i>Nitrospira</i> )	Canonical K-NOB ( <i>Nitrobacter</i> )	Comammox ( <i>Nitrospira</i> )	References
$\mu_{\max}$ (d <sup>-1</sup> )		0.24		0.18		(Liu and Wang 2014)
		0.2-0.9				(Metcalf et al., 2003)
		3.03	1.01	0.93	0.31	(Yu et al., 2020)
		0.54-2.1	0.7-0.9			(Zhang et al., 2019)
b (d <sup>-1</sup> )			0.39-1.28		0.69	(Park et al., 2017)
			2.25-2.51			(Liu et al., 2017)
K <sub>NH4</sub> (mg N/L)		0.09-0.27		0.09-0.27		(Metcalf et al., 2003)
		0.05-0.15		0.05-0.15		(Henze 2000)
K <sub>NO2</sub> (mg N/L)		0.675				(Yu et al., 2020)
		0.225			0.0005	(Sakoula et al., 2021)
				0.765	0.255	(Koch et al., 2019)
		0.076-0.612			0.009	(Kits et al., 2017)
K <sub>O</sub> (mg O <sub>2</sub> /L)						(Yu et al., 2020)
			0.69-7.62	0.126-0.378	5.21	(Nowka et al., 2015)
		0.42	1.35	0.45		(Yu et al., 2020)
Y (mg COD/mg N)			0.13-1.10			(Zhang et al., 2019)
			0.17-4.32		0.33	(Park et al., 2017)
Y (mg COD/mg N)		0.36	0.54			(Liu et al., 2017)
		0.18		0.08		(Jubany et al., 2008)
			0.07-0.14			(Park et al., 2017)
					0.2-0.38	(Kits et al., 2017)
	0.15-0.24					(Eldyasti et al., 2012)

848  $\mu$ : maximum specific growth rate, K: half-saturation coefficient, b: decay coefficient, Y: growth yield coefficient

849





851  
 852 **Figure S2-** Observed vs. predicted relative abundances of comammox bacteria in trial T3 (comammox can growth  
 853 only on  $\text{NH}_4\text{-N}$ )  
 854  
 855

856 **Table S5.** Kinetic and stoichiometric parameters for canonical *Nitrospira*, comammox *Nitrospira*, and *Nitrobacter*  
 857 reported in the literature

Bacteria	$\mu_{\max}$ (d <sup>-1</sup> )	b (d <sup>-1</sup> )	Y (g VSS/g N or g COD/g N)	K <sub>NH4</sub> (mg N/L)	K <sub>NO2</sub> (mg N/L)	K <sub>O</sub> (mg O <sub>2</sub> /L)	Remarks	Reference
<i>Nitrospira</i>								
	0.31	0.02	-		0.25	0.45	T= 17-22 °C, pH=7.5–8.2, Enriched culture	(Yu et al., 2020)
	0.69 ± 0.10	-	0.14 ± 0.02 (g VSS/g N)	-	0.52 ± 0.14	0.33 ± 0.04	T=22 °C, pH=7.5±0.1 Enriched culture, lineage I	(Park et al. 2017)
			0.12 ± 0.04 (g VSS/g N)	-	0.9-1.1	0.54	T=22 °C, pH=7.5 Enriched culture	(Blackburne et al. 2007)
	0.45-0.52	-	-	-	0.13-0.39	-	T=28–37 °C, pH=7.4-8.6 Pure culture, <i>Nitrospira defluvii</i> , and <i>Moscoviensis</i> ,	(Nowka et al. 2015)
	-		-	-	0.08 (Lineage I) 0.14 (Lineage II)	-	T=29°C, Pure culture, <i>Nitrospira</i> lineage I and II	(Ushiki et al. 2017)
	0.45	-	-	-	-	-	T=N/a, Enriched culture	(Lawson and Lücker 2018)
	-	-	-	-	5.21	-	T=37 °C, Pure culture, <i>clade 1</i> , <i>lineage II</i>	(Kits et al. 2017)

0.2	0.04	0.05 (g COD/g N)	0.06	0.13	T=12-20 °C, Mixed culture	This study
-----	------	---------------------	------	------	------------------------------	------------

---

858

Comammox <i>-Nitrospira</i>	0.148	-	-	0.009	-	-	T=N/a, Enriched culture Clade A	(Lawson and Lücker, 2018)
	-	-	-	0.012	6.29	-	T= NA, pH= NA Pure culture, <i>lineage II</i>	(Koch et al. 2019)
	-	-	-	0.0005	0.175	-	-	(Sakoula et al., 2021)
	0.2	0.04	0.15 (g COD/g N)	-	-	-	T=12-20 °C, Mixed culture Clade A	This study
<i>Nitrobacter</i>	0.93	0.05	-	-	0.76	1.35	T= 17-22 °C, pH=7.5–8.2, Enriched culture	(Yu et al., 2020)
	-	-	0.08 (g VSS/g N)	-	1.2–1.3	0.43	T=22 °C, Enriched culture,	(Blackburne et al., 2007)
	0.39–1.28	-	-	-	0.69–7.6	-	T= 28–37 °C pH=7.4-8.6, Pure culture	(Nowka et al., 2015)
	-	-	-	-	-	0.17–4.32	T=25 °C, pH=7.3-8.2, Pure culture	(Laanbroek et al., 1994)
	0.48	-	0.07–0.1 (g VSS/g N)	-	1.49	-	T=22 °C, pH=7.3, Mixed culture	(Vadivelu et al., 2006)
	0.6	0.08	0.05 (g COD/g N)	-	0.06	0.45	-	This study
	-	-	-	-	-	-	-	-

859  $\mu_{\max}$ : Maximum growth rate, Y: Yield coefficient, Ko: DO affinity constant,  $K_{\text{NH}_4}$ : Ammonia affinity constant,  $K_{\text{NO}_2}$ :

860 Nitrite affinity constant,

861

862



863 **References**

- 864 Blackburne R, Vadivelu VM, Yuan Z, Keller J. Kinetic characterisation of an enriched *Nitrospira*  
865 culture with comparison to *Nitrobacter*. *Water Research* 2007; 41: 3033-3042.  
866
- 867 Eldyasti, A., Nakhla, G. and Zhu, J., 2012. Development of a calibration protocol and  
868 identification of the most sensitive parameters for the particulate biofilm models used in  
869 biological wastewater treatment. *Bioresource Technology* 111, 111-121.  
870 10.1016/j.biortech.2012.02.021  
871
- 872 Henze, M.G., W., Mino, T., van Loosdrecht, M.C.M. (2000) *Activated sludge models ASM1,*  
873 *ASM2, ASM2d and ASM3*, IWA Publishing, London, UK.  
874
- 875 Jubany, I., Carrera, J., Lafuente, J. and Baeza, J.A., 2008. Start-up of a nitrification system with  
876 automatic control to treat highly concentrated ammonium wastewater: Experimental results  
877 and modeling. *Chemical Engineering Journal* 144(3), 407-419. 10.1016/j.cej.2008.02.010  
878
- 879 Kits, K.D., Sedlacek, C.J., Lebedeva, E.V., Han, P., Bulaev, A., Pjevac, P., Daebeler, A.,  
880 Romano, S., Albertsen, M., Stein, L.Y., Daims, H. and Wagner, M., 2017. Kinetic analysis  
881 of a complete nitrifier reveals an oligotrophic lifestyle. *Nature* 549(7671), 269-272.  
882 10.1038/nature23679  
883
- 884 Koch, H., van Kessel, M.A.H.J. and Lücker, S., 2019. Complete nitrification: insights into the  
885 ecophysiology of comammox *Nitrospira*. *Applied Microbiology and Biotechnology* 103(1),  
886 177-189. 10.1007/s00253-018-9486-3  
887
- 888 Klindworth, A., Pruesse, E., Schweer, T., Peplies, J., Quast, C., Horn, M. and Glöckner, F.O.,  
889 2012. Evaluation of general 16S ribosomal RNA gene PCR primers for classical and next-  
890 generation sequencing-based diversity studies. *Nucleic Acids Research* 41(1), e1-e1.  
891 10.1093/nar/gks808  
892
- 893 Liu, G. and Wang, J., 2014. Role of Solids Retention Time on Complete Nitrification:  
894 Mechanistic Understanding and Modeling. *Journal of Environmental Engineering* 140(1),  
895 48-56. 10.1061/(ASCE)EE.1943-7870.0000779  
896
- 897 Meyer, F., Paarmann, D., D'Souza, M., Olson, R., Glass, E.M., Kubal, M., Paczian, T.,  
898 Rodriguez, A., Stevens, R., Wilke, A., Wilkening, J. and Edwards, R.A., 2008. The  
899 metagenomics RAST server – a public resource for the automatic phylogenetic and  
900 functional analysis of metagenomes. *BMC Bioinformatics* 9(1), 386-399. 10.1186/1471-  
901 2105-9-386  
902
- 903 Laanbroek HJ, Bodelier PLE, Gerards S. Oxygen consumption kinetics of *Nitrosomonas*  
904 *europaea* and *Nitrobacter hamburgensis* grown in mixed continuous cultures at different  
905 oxygen concentrations. *Archives of Microbiology* 1994; 161: 156-162.  
906
- 907 Lawson CE, Lücker S. Complete ammonia oxidation: an important control on nitrification in  
908 engineered ecosystems? *Current Opinion in Biotechnology* 2018; 50: 158-165.

- 909  
910 Liu, J., Wu, Y., Wu, C., Muylaert, K., Vyverman, W., Yu, H.-Q., Muñoz, R. and Rittmann, B.,  
911 2017. Advanced nutrient removal from surface water by a consortium of attached  
912 microalgae and bacteria: A review. *Bioresource Technology* 241, 1127-1137.  
913 10.1016/j.biortech.2017.06.054  
914  
915 Metcalf and Eddy, Inc. 2003. *Wastewater engineering : treatment and reuse*, Fourth edition /  
916 revised by George Tchobanoglous, Franklin L. Burton, H. David Stensel. Boston :  
917 McGraw-Hill, 2003.  
918  
919 Nowka, B., Daims, H. and Spieck, E., 2015. Comparison of Oxidation Kinetics of Nitrite-  
920 Oxidizing Bacteria: Nitrite Availability as a Key Factor in Niche Differentiation. *Applied*  
921 *and Environmental Microbiology* 81(2), 745. 10.1128/AEM.02734-14  
922  
923 Park, M.-R., Park, H. and Chandran, K., 2017. Molecular and Kinetic Characterization of  
924 Planktonic *Nitrospira* spp. Selectively Enriched from Activated Sludge. *Environmental*  
925 *Science & Technology* 51(5), 2720-2728. 10.1021/acs.est.6b05184  
926  
927 Pjevac, P., Schaubberger, C., Poghosyan, L., Herbold, C.W., van Kessel, M.A.H.J., Daebeler, A.,  
928 Steinberger, M., Jetten, M.S.M., Lücker, S., Wagner, M. and Daims, H., 2017. AmoA-  
929 Targeted Polymerase Chain Reaction Primers for the Specific Detection and Quantification  
930 of Comammox *Nitrospira* in the Environment. *Frontiers in Microbiology* 8(1508).  
931 10.3389/fmicb.2017.01508  
932  
933 Sakoula, D., Koch, H., Frank, J., Jetten, M.S.M., van Kessel, M.A.H.J. and Lücker, S., 2021.  
934 Enrichment and physiological characterization of a novel comammox *Nitrospira* indicates  
935 ammonium inhibition of complete nitrification. *The ISME Journal* 15(4), 1010-1024.  
936 10.1038/s41396-020-00827-4  
937  
938 Vadivelu VM, Yuan Z, Fux C, Keller J. 2006. Stoichiometric and kinetic characterisation of  
939 *Nitrobacter* in mixed culture by decoupling the growth and energy generation processes.  
940 *Biotechnology and Bioengineering* 94: 1176-1188.  
941  
942 Yu, L., Chen, S., Chen, W. and Wu, J., 2020. Experimental investigation and mathematical  
943 modeling of the competition among the fast-growing “r-strategists” and the slow-growing  
944 “K-strategists” ammonium-oxidizing bacteria and nitrite-oxidizing bacteria in nitrification.  
945 *Science of The Total Environment* 702, 135049. 10.1016/j.scitotenv.2019.135049  
946  
947 Zhang, D., Su, H., Antwi, P., Xiao, L., Liu, Z. and Li, J., 2019. High-rate partial-nitrification and  
948 efficient nitrifying bacteria enrichment/out-selection via pH-DO controls: Efficiency,  
949 kinetics, and microbial community dynamics. *Science of The Total Environment* 692, 741-  
950 755. 10.1016/j.scitotenv.2019.07.308  
951  
952

953

